



Aerothermal Database for Off-Nominal Earth Reentry of the Dragonfly Aeroshell.

Presented by: Christopher Naughton

Christopher Naughton, Aaron Brandis
NASA Ames Research Center

David Saunders
AMA Inc., NASA Ames Research Center

Don Li, Shervin Taghavi, Elan Borenstein
Jet Propulsion Laboratory



THERMAL & FLUIDS
ANALYSIS WORKSHOP
Ames Research Center 2025

Thermal & Fluids Analysis Workshop 2025
NASA Ames Research Center

San Jose, CA
August 4-7, 2025



Introduction



Dragonfly is an upcoming New Frontiers mission sending an autonomous rotorcraft to Saturn's moon Titan.

- Rotorcraft will study Titan's prebiotic chemistry.

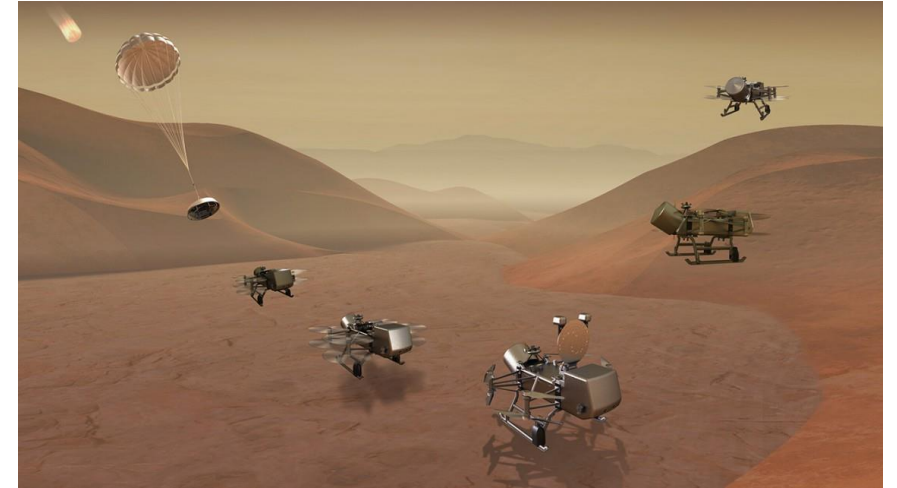
Lander is powered by a Multi-Mission Radioisotope Thermoelectric Generator (MMRTG).

- Needed due to Titan's atmosphere & distance from Sun.
- Similar design to the MMRTG on the Mars2020 rover.

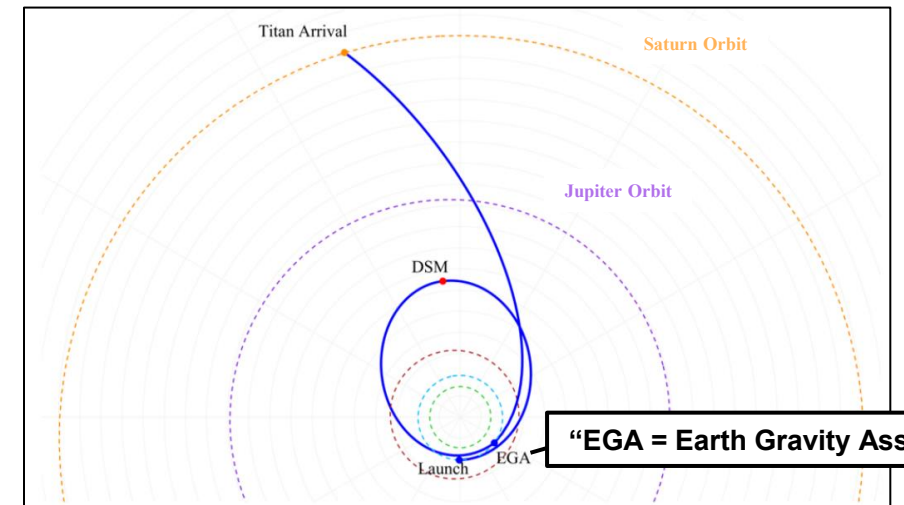
Launching a nuclear power source (NPS) requires safety analysis evaluating risk from accidental Earth re-entry [1].

- Possible failure scenarios: (1) Suborbital launch failure, (2) Orbital decay from LEO and (3) Earth gravity assist mistarget.

Dragonfly team is assembling a novel aerothermal database for off-nominal Earth reentries.



Dragonfly Mission Concept Art



Sample Dragonfly Interplanetary Trajectory Using an Earth Gravity Assist [2]

“EGA = Earth Gravity Assist”



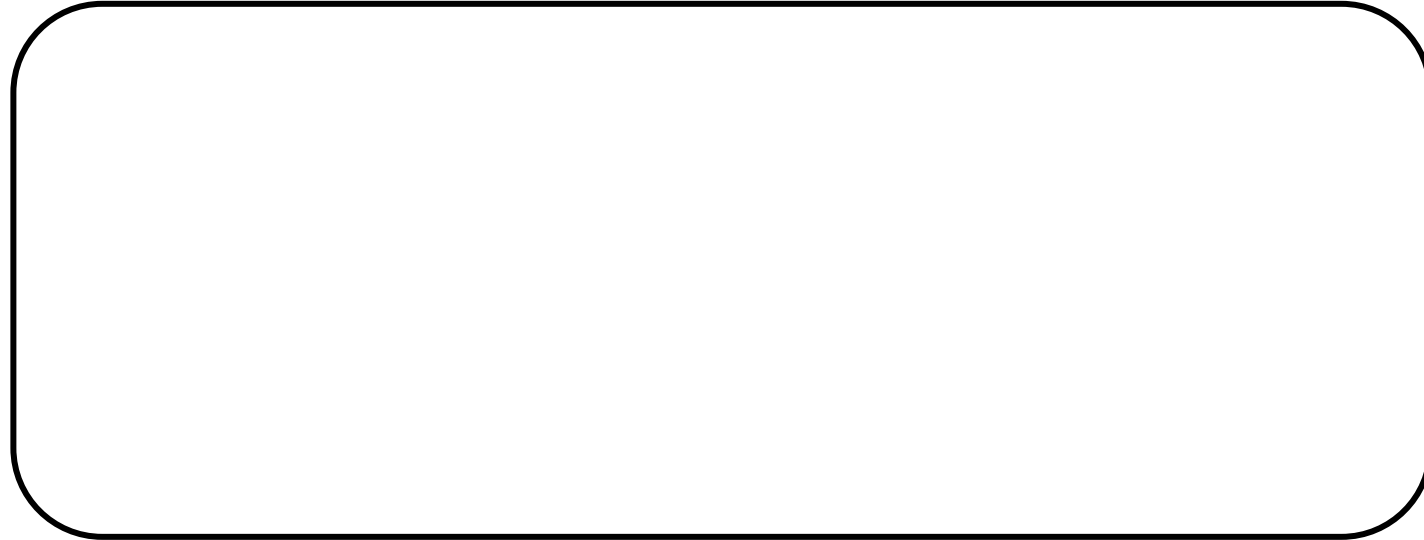
Nuclear Safety Analysis



Entry aerothermal analysis is used in two primary components of nuclear safety analysis:

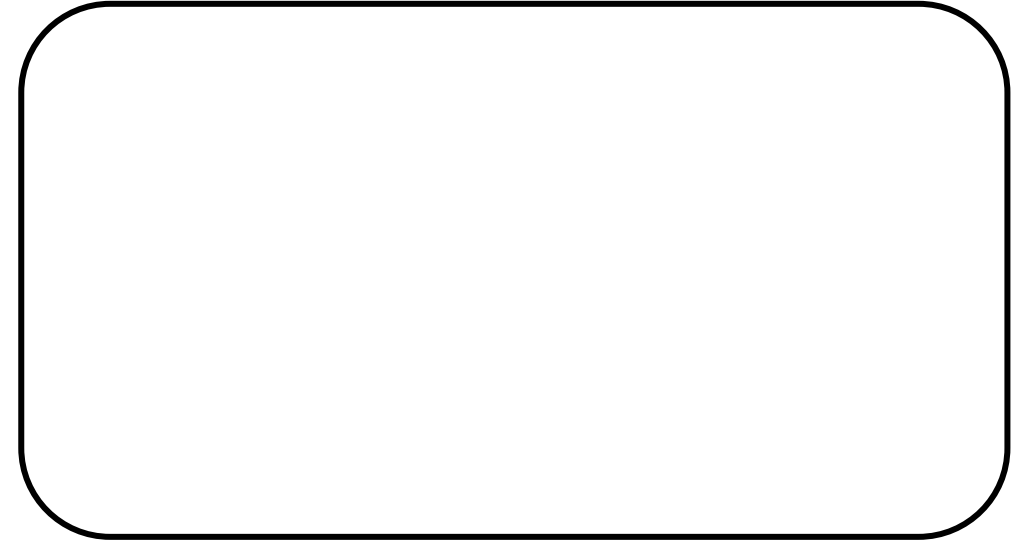
- 1) Launch Authorization Process – Assess radiological risk and inform decision makers.**
- 2) Radioisotope Contingency Planning (RCP) – Real-time monitoring and footprint assessments.**

Launch Authorization Process



NOTE: Full launch authorization has more steps than the above process; only the components directly involving entry aerothermal analysis are shown.

Radioisotope Contingency Planning



NOTE: RCP has more steps than the above process; only the components directly involving entry aerothermal analysis are shown.



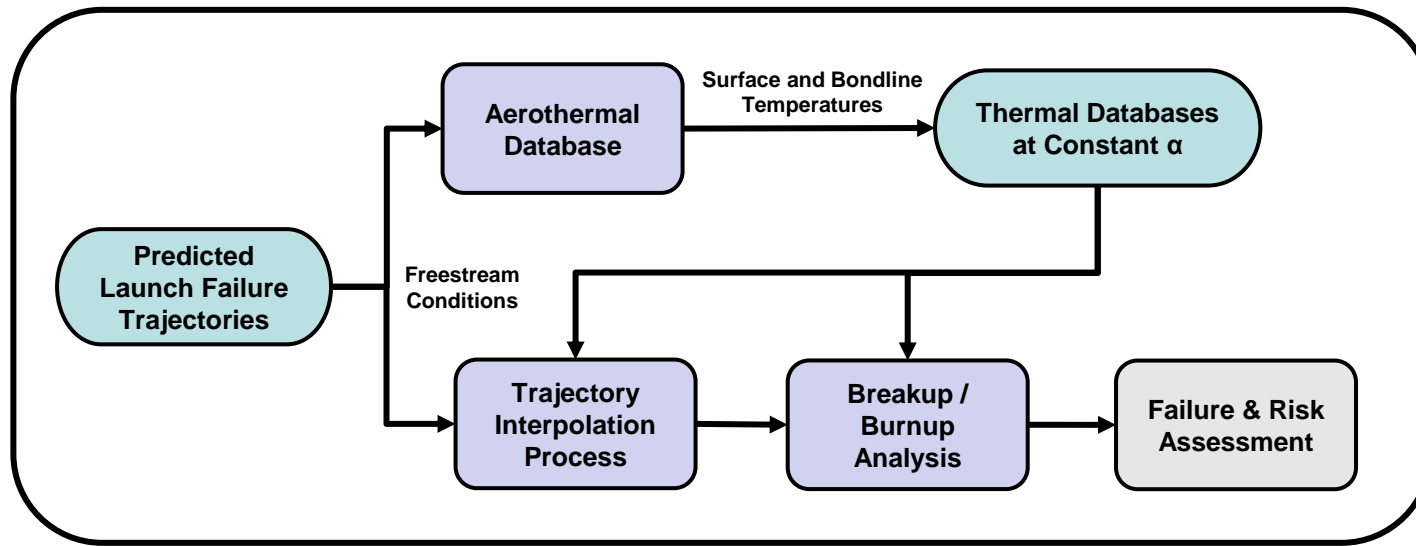
Nuclear Safety Analysis



Entry aerothermal analysis is used in two primary components of nuclear safety analysis:

- 1) **Launch Authorization Process** – Assess radiological risk and inform decision makers.
- 2) **Radioisotope Contingency Planning (RCP)** – Real-time monitoring and footprint assessments.

Launch Authorization Process



NOTE: Full launch authorization has more steps than the above process; only the components directly involving entry aerothermal analysis are shown.

Radioisotope Contingency Planning



NOTE: RCP has more steps than the above process; only the components directly involving entry aerothermal analysis are shown.



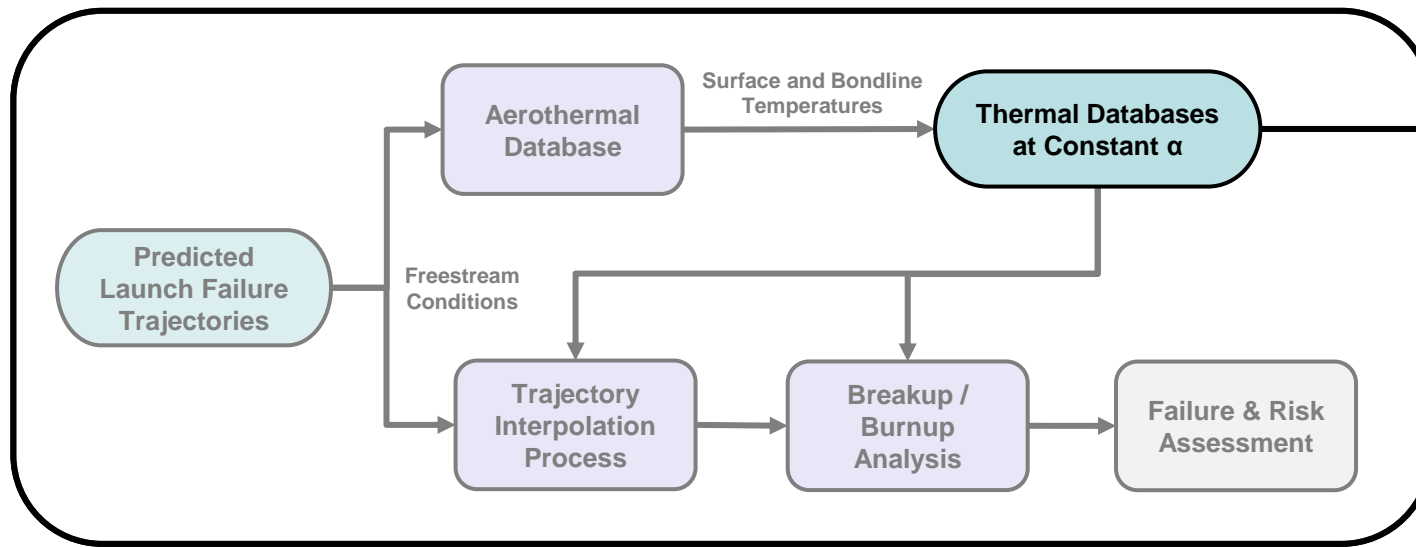
Nuclear Safety Analysis



Entry aerothermal analysis is used in two primary components of nuclear safety analysis:

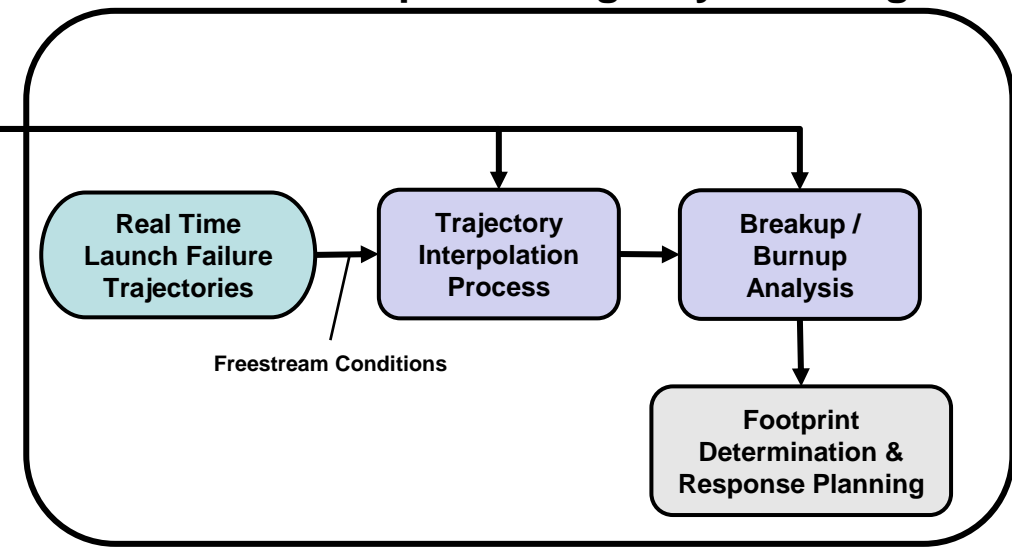
- 1) Launch Authorization Process – Assess radiological risk and inform decision makers.
- 2) Radioisotope Contingency Planning (RCP) – Real-time monitoring and footprint assessments.

Launch Authorization Process



NOTE: Full launch authorization has more steps than the above process; only the components directly involving entry aerothermal analysis are shown.

Radioisotope Contingency Planning



NOTE: RCP has more steps than the above process; only the components directly involving entry aerothermal analysis are shown.



Nuclear Safety Analysis



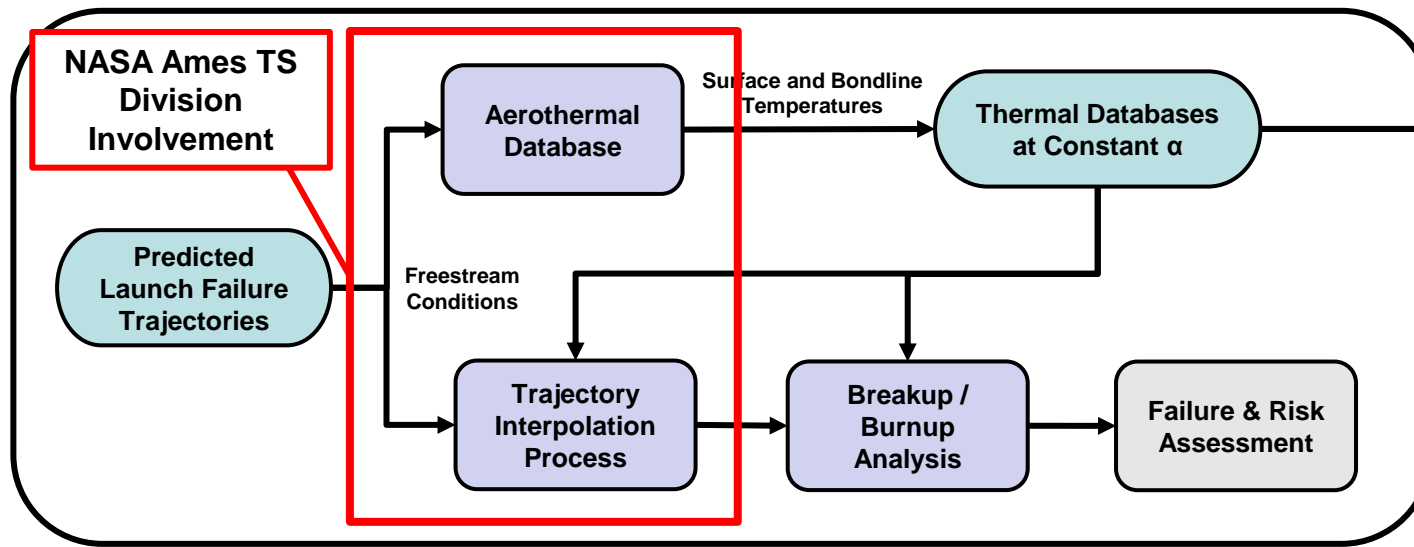
Entry aerothermal analysis is used in two primary components of nuclear safety analysis:

- 1) **Launch Authorization Process** – Assess radiological risk and inform decision makers.
- 2) **Radioisotope Contingency Planning (RCP)** – Real-time monitoring and footprint assessments.

Both components use databases of *surface heat fluxes* and *in-depth temperatures*.

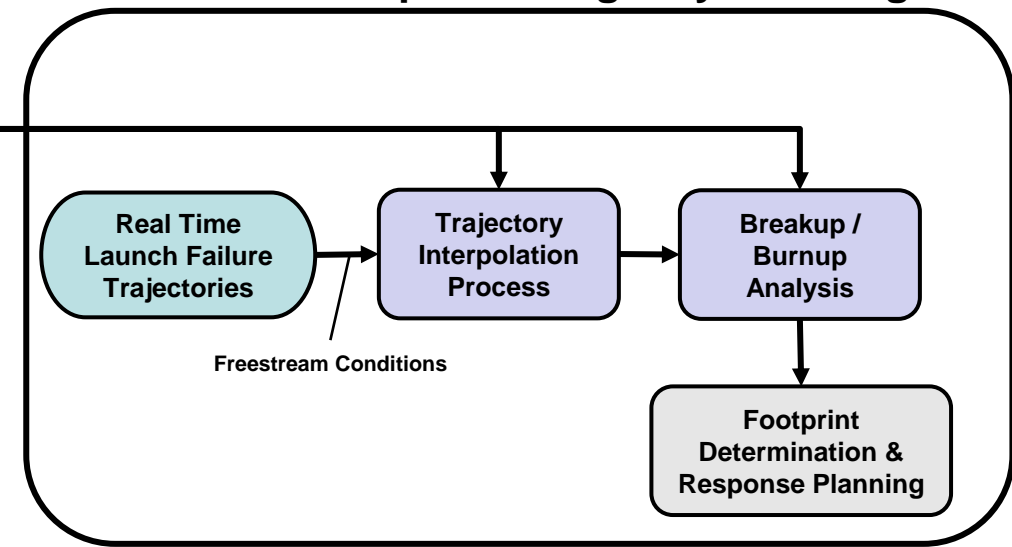
- Past efforts looked at 2x angles of attack (0°, 180°) and used the closest previously-simulated trajectory.
- Current effort is developing a more sophisticated data-fusion methodology (*in progress*)

Launch Authorization Process



NOTE: Full launch authorization has more steps than the above process; only the components directly involving entry aerothermal analysis are shown.

Radioisotope Contingency Planning



NOTE: RCP has more steps than the above process; only the components directly involving entry aerothermal analysis are shown.

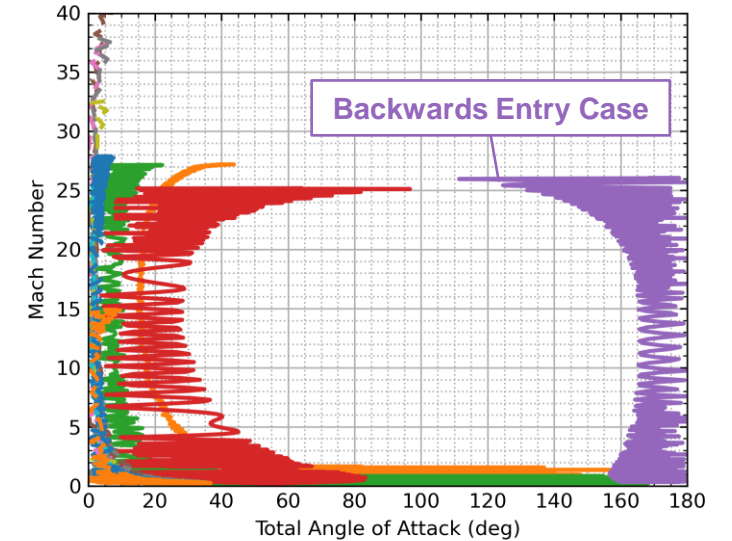


Aerothermal Database - Design



Accidental re-entry thermal analysis has unique requirements.

- Capsule may enter backwards ($\alpha \approx 180^\circ$) or tumbling ($\alpha \leq 180^\circ$).
- Lower altitude failure is *worse*; lower heating may be conservative.



Preliminary Trajectories Showing a Backwards Entry ($\alpha \approx 180^\circ$)



Aerothermal Database - Design

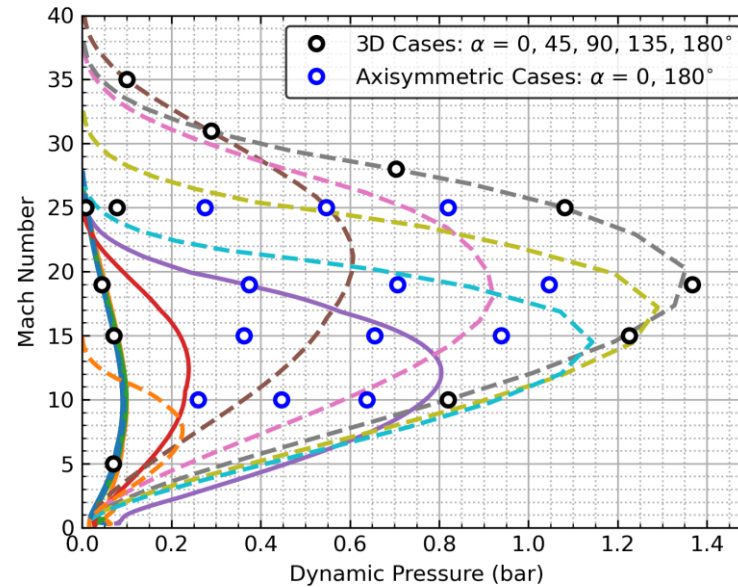


Accidental re-entry thermal analysis has unique requirements.

- Capsule may enter backwards ($\alpha \approx 180^\circ$) or tumbling ($\alpha \leq 180^\circ$).
- Lower altitude failure is *worse*; lower heating may be conservative.

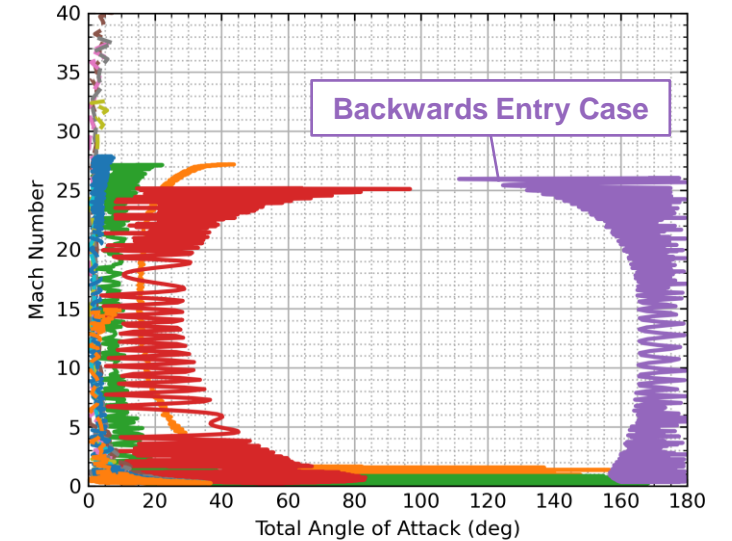
Use CBAERO [3] with CFD to predict environments.

- CBAERO interpolates in M-Q- α space & can be anchored to CFD.
- Develop independent databases at constant α - [0, 45, 90, 135, 180] $^\circ$.

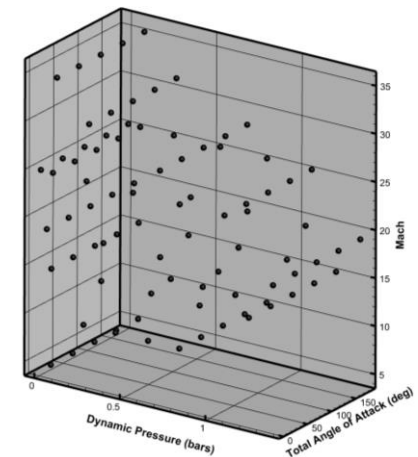


Trajectories in CBAERO Interpolation Space w/ High-Fidelity CFD

TFAWS 2025 – August 4-7, 2025



Preliminary Trajectories Showing a Backwards Entry ($\alpha \approx 180^\circ$)



Full Set of High-Fidelity CFD



Aerothermal Database - Design

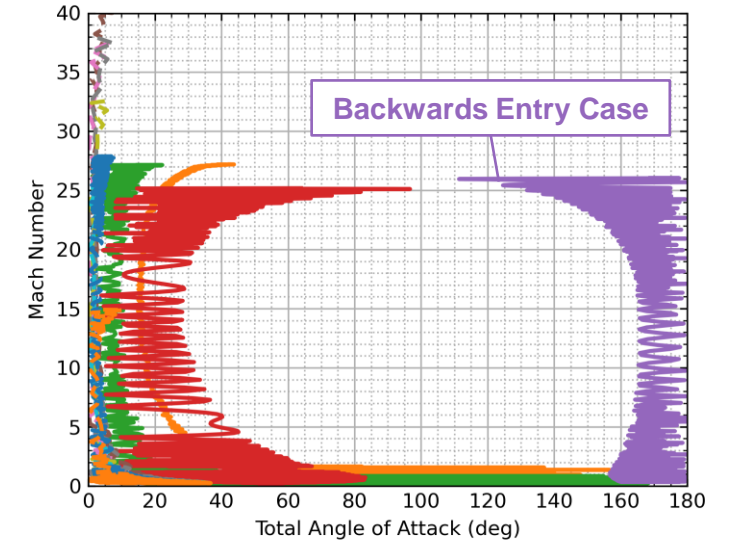


Accidental re-entry thermal analysis has unique requirements.

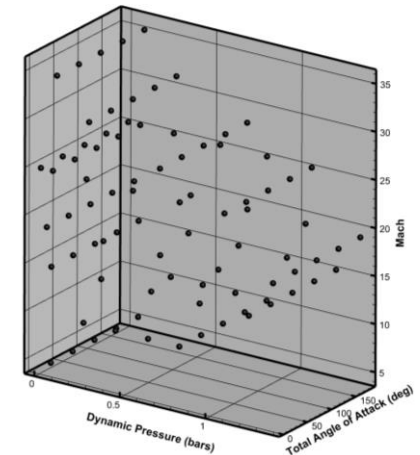
- Capsule may enter backwards ($\alpha \approx 180^\circ$) or tumbling ($\alpha \leq 180^\circ$).
- Lower altitude failure is *worse*; lower heating may be conservative.

Use CBAERO [3] with CFD to predict environments.

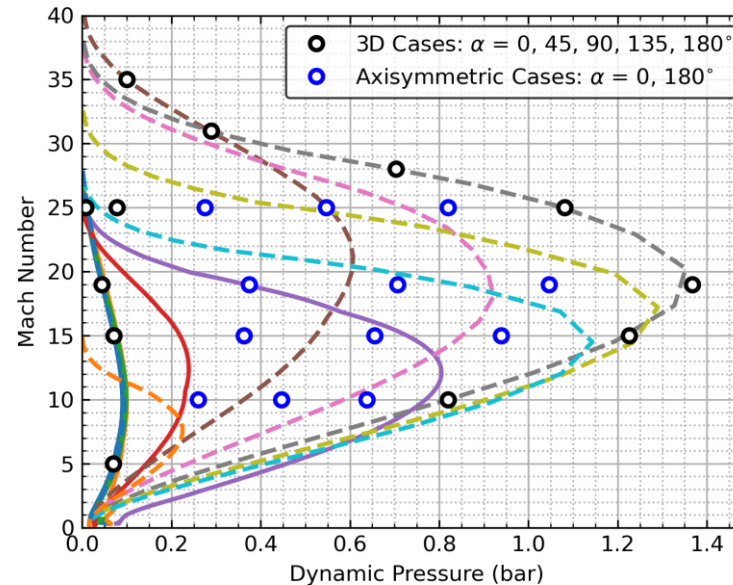
- CBAERO interpolates in M-Q- α space & can be anchored to CFD.
- Develop independent databases at constant α - [0, 45, 90, 135, 180] $^\circ$.



Preliminary Trajectories Showing a Backwards Entry ($\alpha \approx 180^\circ$)



Full Set of High-Fidelity CFD



Trajectories in CBAERO Interpolation Space w/ High-Fidelity CFD

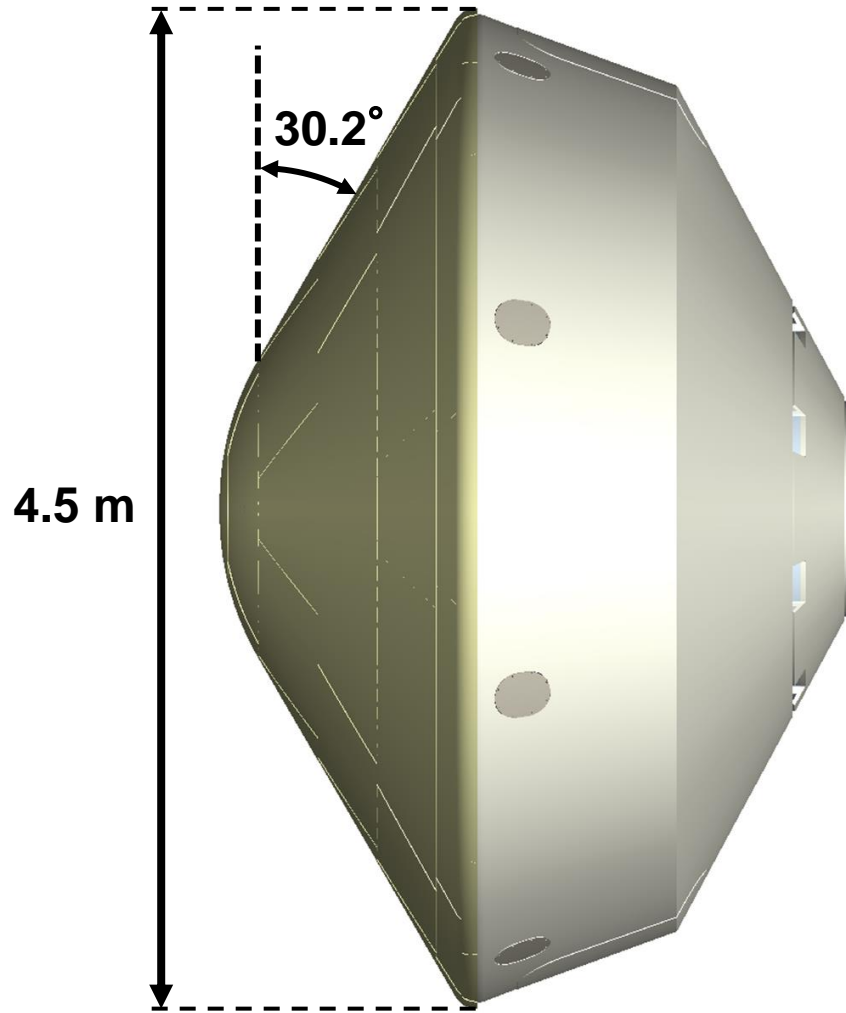
Database Overview

Each database is anchored to high fidelity CFD.

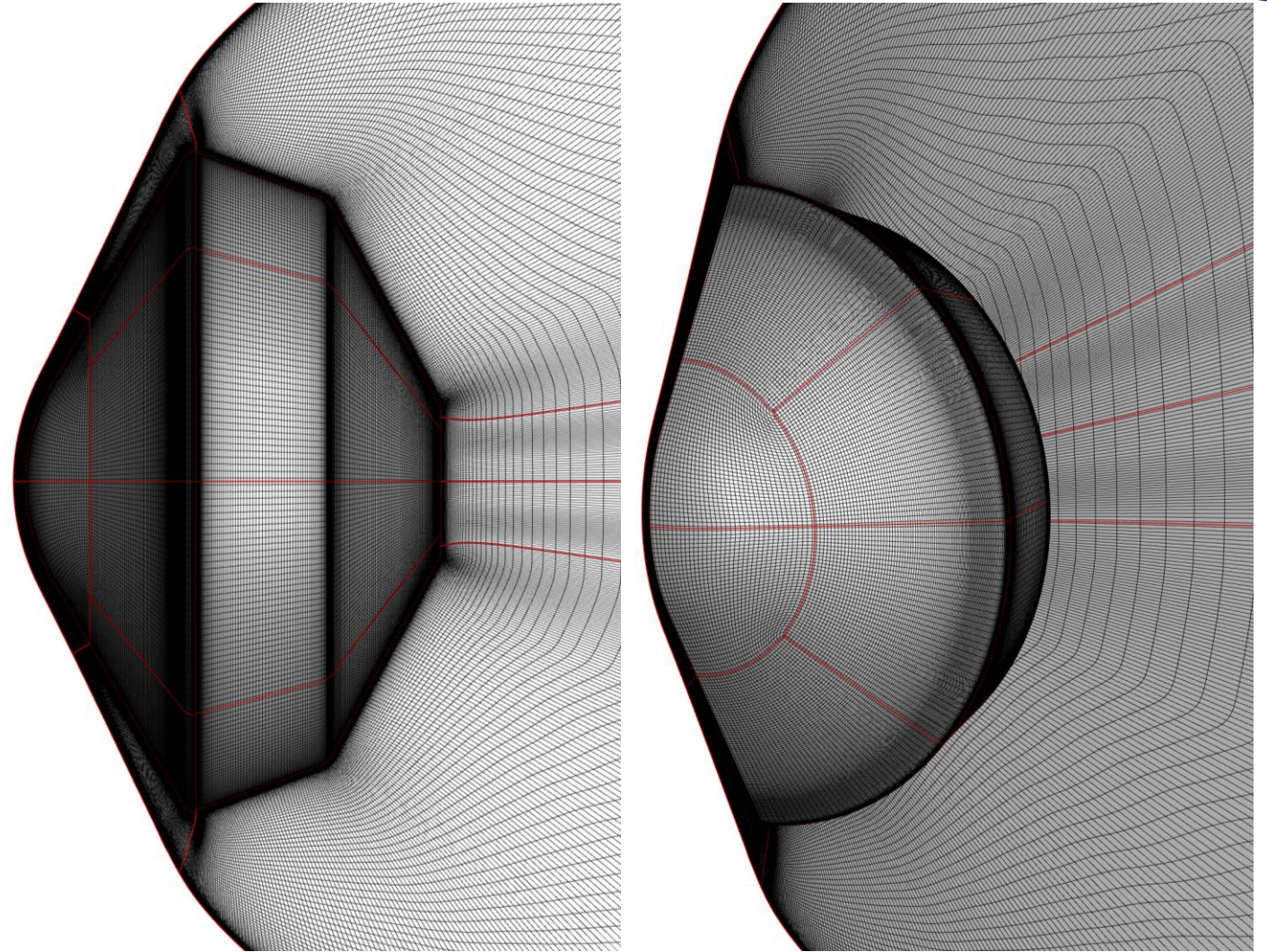
- 24x CFD cases for $\alpha = [0, 180]^\circ$.
- 12x CFD cases for $\alpha = [45, 90, 135]^\circ$.
- 84x total CFD cases.



Capsule Geometry and Mesh



Dragonfly Aeroshell Geometry
(4.5 m, 60° Sphere-Cone)



Example CFD Mesh - Surface and Shock-Aligned Pitch-Plane
(Halfbody, 5.3×10^4 Surface Quad Cells, 6.4×10^6 Volume Hex Cells)



CFD Modeling



All CFD cases are run with DPLR [5] and include thermal and chemical nonequilibrium.

- **Use 7 and 11 species chemistry models (N_2 , O_2 , NO , NO^+ , N , O , e^- ; & N_2^+ , O_2^+ , N^+ , O^+ for radiation).**
- **Both Laminar and Fully-Turbulent with the Menter-SST (Shear Stress Transport) turbulence model.**



CFD Modeling

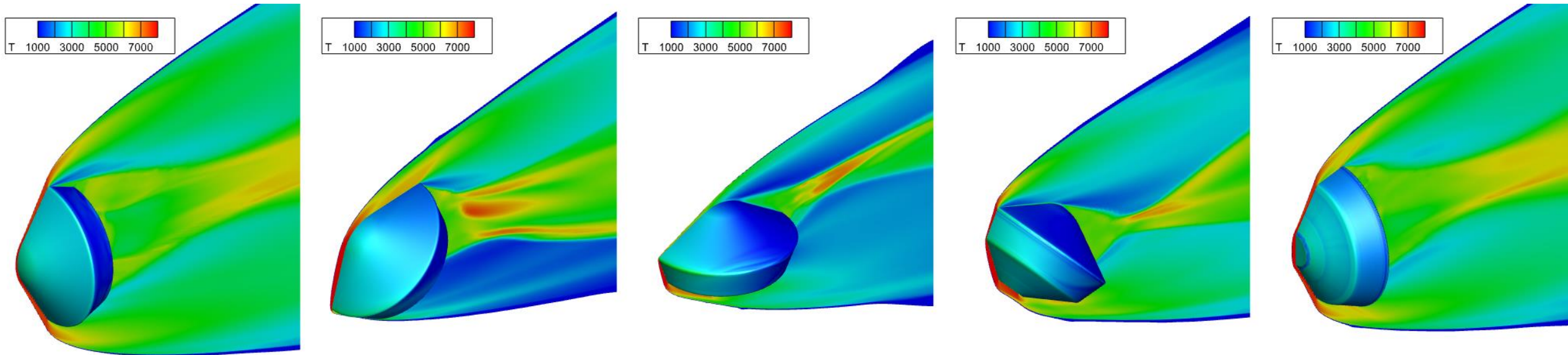


All CFD cases are run with DPLR [5] and include thermal and chemical nonequilibrium.

- Use 7 and 11 species chemistry models (N_2 , O_2 , NO , NO^+ , N , O , e^- ; & N_2^+ , O_2^+ , N^+ , O^+ for radiation).
- Both Laminar and Fully-Turbulent with the Menter-SST (Shear Stress Transport) turbulence model.

Previous work (MSL [4]) used simplifying assumptions.

- Ran axisymmetric CFD at $[0, 180]^\circ \rightarrow$ Now at $[0, 45, 90, 135, 180]^\circ$.
- Laminar assumed to be conservative \rightarrow Now incorporate turbulent transition.
- No radiative heating anchoring \rightarrow Predict radiative heat flux for $U_\infty > 7$ km/s.



Pitch-Plane and Wall Temperature Contours at Database Angles of Attack ($U_\infty = 9.2$ km/s, $\rho_\infty = 1.7 \times 10^{-3}$ kg/m³)



Turbulent Transition



Neither laminar nor turbulent are always “conservative”.

- **Failing late in the trajectory is worse than earlier.**



Turbulent Transition

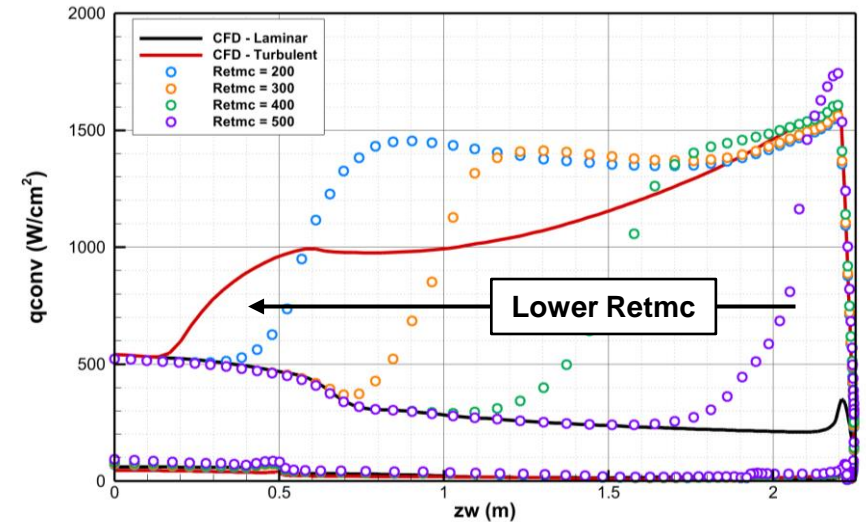


Neither laminar nor turbulent are always “conservative”.

- Failing late in the trajectory is worse than earlier.

CBAERO has a transition model whose input transition parameter (“Retmc”) roughly correlates with Re_θ .

- $Re_\theta = \frac{\rho_e U_e \theta}{\mu_e}$, e = Thermal boundary layer edge
- Anchor momentum thickness (θ) to CFD cases.
- Select a transition criterion of $Re_\theta \approx 200$ based on a study for the MSL aeroshell geometry [6].



Impact of CBAERO Transition Parameter on Heating ($U_\infty = 8.0$ km/s, $\rho_\infty = 3.4 \times 10^{-3}$ kg/m³).



Turbulent Transition



Neither laminar nor turbulent are always “conservative”.

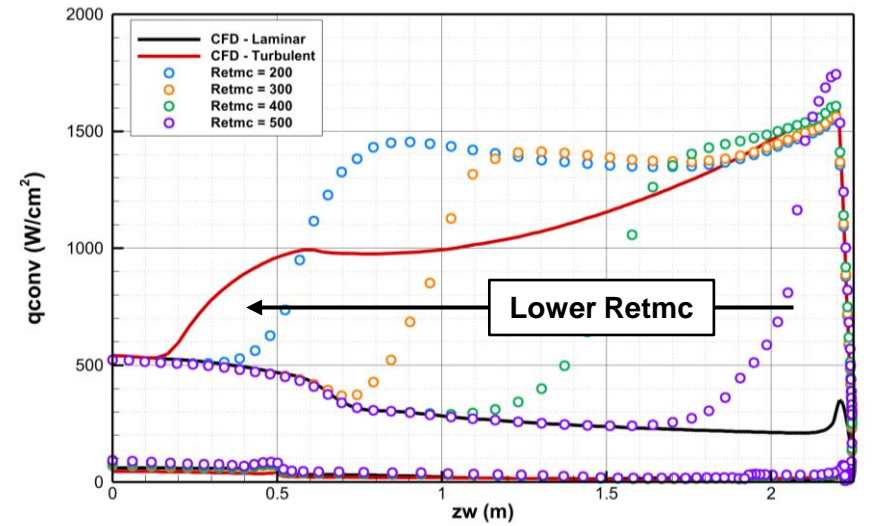
- Failing late in the trajectory is worse than earlier.

CBAERO has a transition model whose input transition parameter (“Retmc”) roughly correlates with Re_θ .

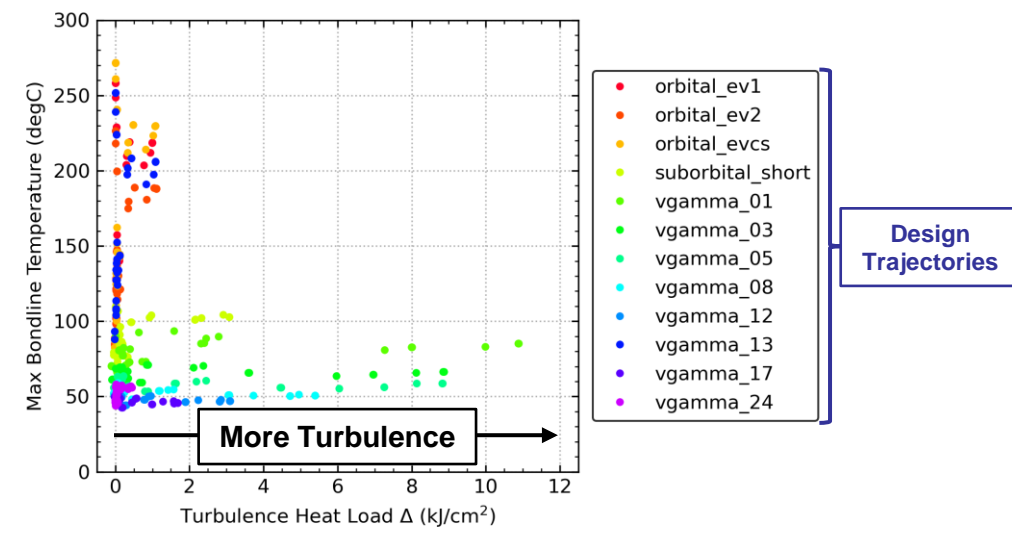
- $Re_\theta = \frac{\rho_e U_e \theta}{\mu_e}$, e = Thermal boundary layer edge
- Anchor momentum thickness (θ) to CFD cases.
- Select a transition criterion of $Re_\theta \approx 200$ based on a study for the MSL aeroshell geometry [6].

Trajectories most impacted by turbulence don’t result in the highest bondline temps.

- Faster entry → Shorter Pulse Width → Cooler Bondline



Impact of CBAERO Transition Parameter on Heating ($U_\infty = 8.0$ km/s, $\rho_\infty = 3.4 \times 10^{-3}$ kg/m³).



Highly Turbulent Trajectories are Not Bounding Cases ($\alpha = 0^\circ$ Results)



Turbulent Transition



Neither laminar nor turbulent are always “conservative”.

- Failing late in the trajectory is worse than earlier.

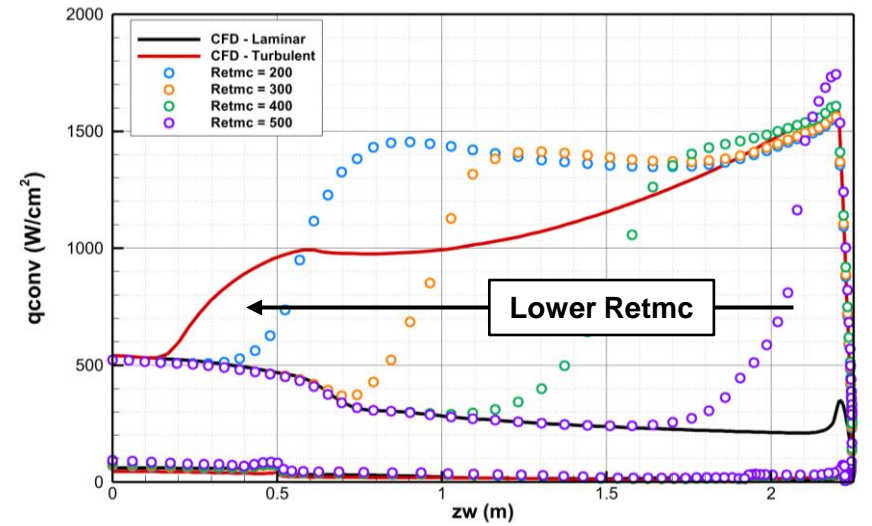
CBAERO has a transition model whose input transition parameter (“Retmc”) roughly correlates with Re_θ .

- $Re_\theta = \frac{\rho_e U_e \theta}{\mu_e}$, e = Thermal boundary layer edge
- Anchor momentum thickness (θ) to CFD cases.
- Select a transition criterion of $Re_\theta \approx 200$ based on a study for the MSL aeroshell geometry [6].

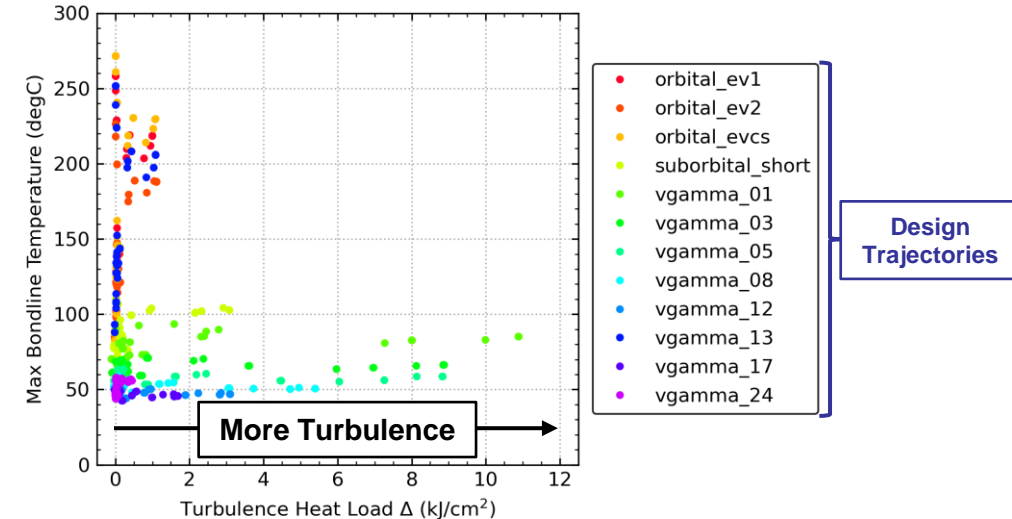
Trajectories most impacted by turbulence don’t result in the highest bondline temps.

- Faster entry → Shorter Pulse Width → Cooler Bondline

Turbulent heating is not a significant driver.



Impact of CBAERO Transition Parameter on Heating ($U_\infty = 8.0$ km/s, $\rho_\infty = 3.4 \times 10^{-3}$ kg/m³).



Highly Turbulent Trajectories are Not Bounding Cases ($\alpha = 0^\circ$ Results)

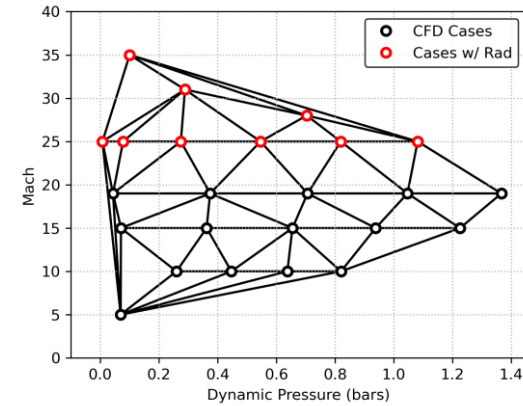


Radiative Heating – Solutions



Include radiation predictions for all cases where $U_{\infty} > 7$ km/s.

- 6x 3D cases (each at 5x α), 3x 2D cases (each at 2x α).



(Left) $\alpha=0^\circ$ Database
with Radiation
Cases Highlighted
($U_{\infty} > 7$ km/s)



Radiative Heating – Solutions

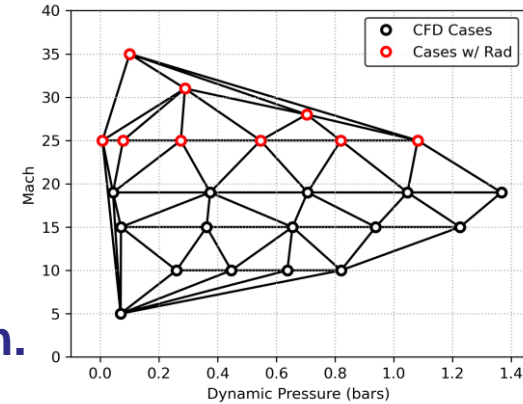


Include radiation predictions for all cases where $U_\infty > 7$ km/s.

- 6x 3D cases (each at 5x α), 3x 2D cases (each at 2x α).

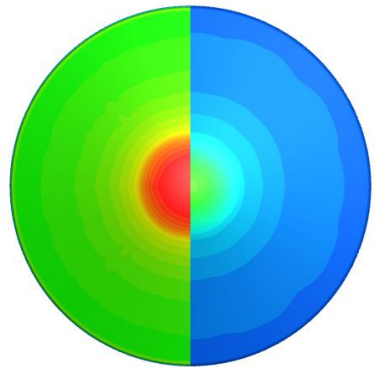
Use the nonequilibrium radiation solver NERO [7].

- NEQAIR is too computationally expensive for spatial resolution.
- Full vehicle NERO solution has similar cost to 1x NEQAIR location.
- NERO agrees well with NEQAIR across flight space.



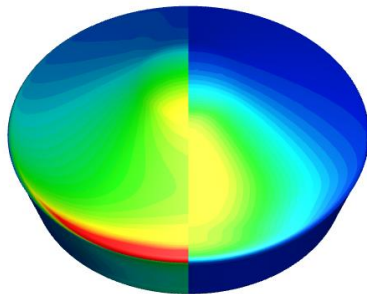
(Left) $\alpha=0^\circ$ Database with Radiation Cases Highlighted ($U_\infty > 7$ km/s)

$\alpha = 0^\circ$



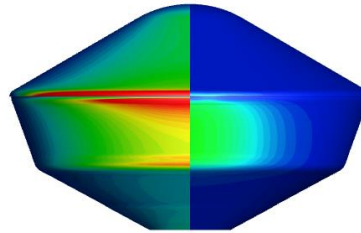
Convective Radiative

$\alpha = 45^\circ$



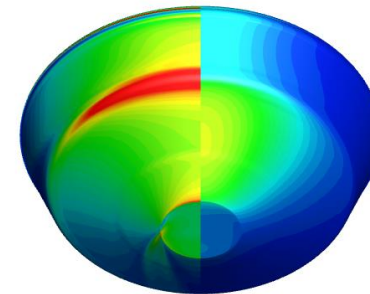
Convective Radiative

$\alpha = 90^\circ$



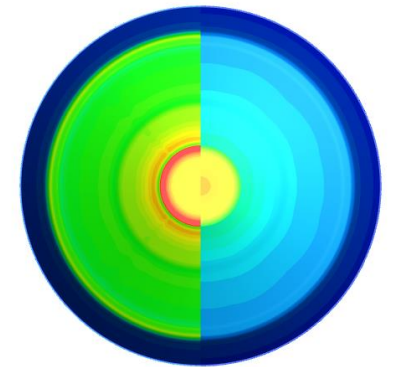
Convective Radiative

$\alpha = 135^\circ$

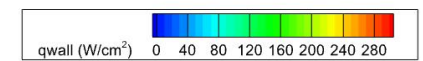
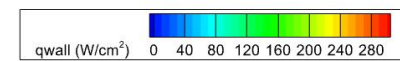
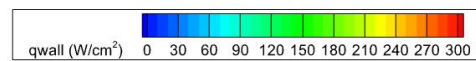
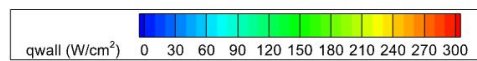
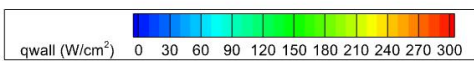


Convective Radiative

$\alpha = 180^\circ$



Convective Radiative



Wall Heat Flux Contours at Database Angles of Attack ($U_\infty = 10.7$ km/s, $\rho_\infty = 1.7 \times 10^{-4}$ kg/m³)



Radiative Heating – Solutions

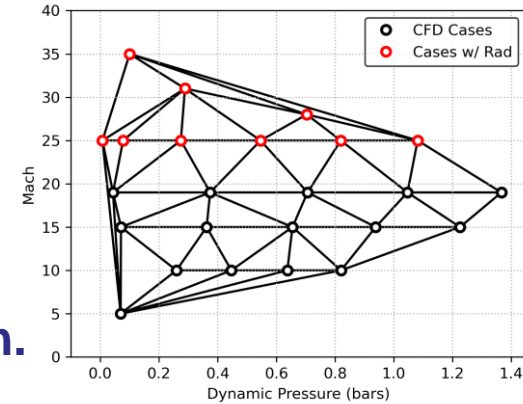


Include radiation predictions for all cases where $U_\infty > 7$ km/s.

- 6x 3D cases (each at 5x α), 3x 2D cases (each at 2x α).

Use the nonequilibrium radiation solver NERO [7].

- NEQAIR is too computationally expensive for spatial resolution.
- Full vehicle NERO solution has similar cost to 1x NEQAIR location.
- NERO agrees well with NEQAIR across flight space.



(Left) $\alpha=0^\circ$ Database with Radiation Cases Highlighted ($U_\infty > 7$ km/s)

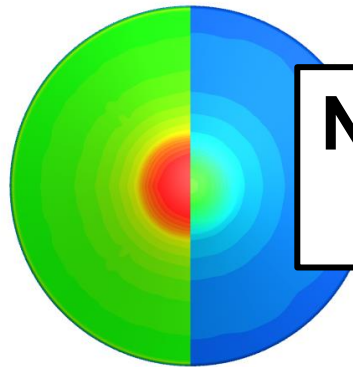
$\alpha = 0^\circ$

$\alpha = 45^\circ$

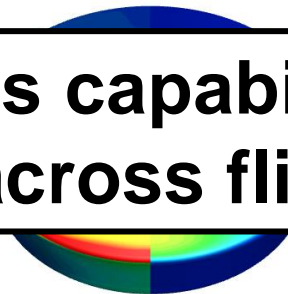
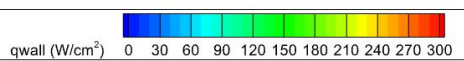
$\alpha = 90^\circ$

$\alpha = 135^\circ$

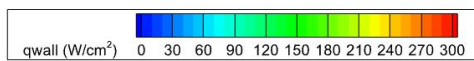
$\alpha = 180^\circ$



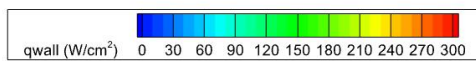
Convective Radiative



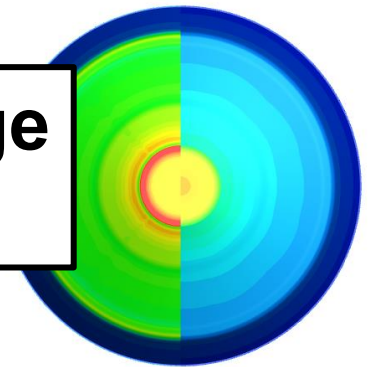
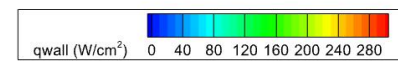
Convective Radiative



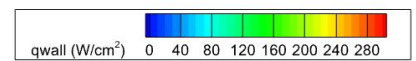
Convective Radiative



Convective Radiative



Convective Radiative



NERO's capabilities enable full database coverage across flight space and angle of attack.

Wall Heat Flux Contours at Database Angles of Attack ($U_\infty = 10.7$ km/s, $\rho_\infty = 1.7 \times 10^{-4}$ kg/m³)



Material Response Modeling

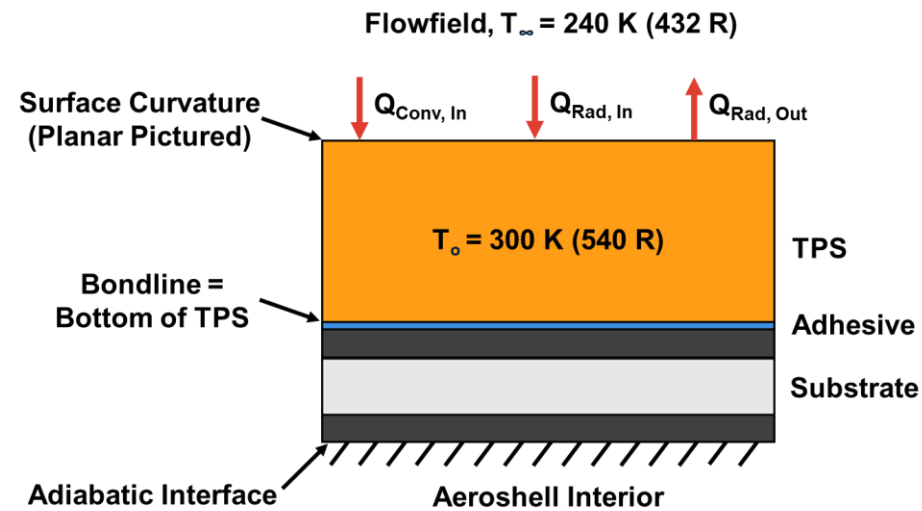


Send CBAERO heating to the material response solver FIAT [8].

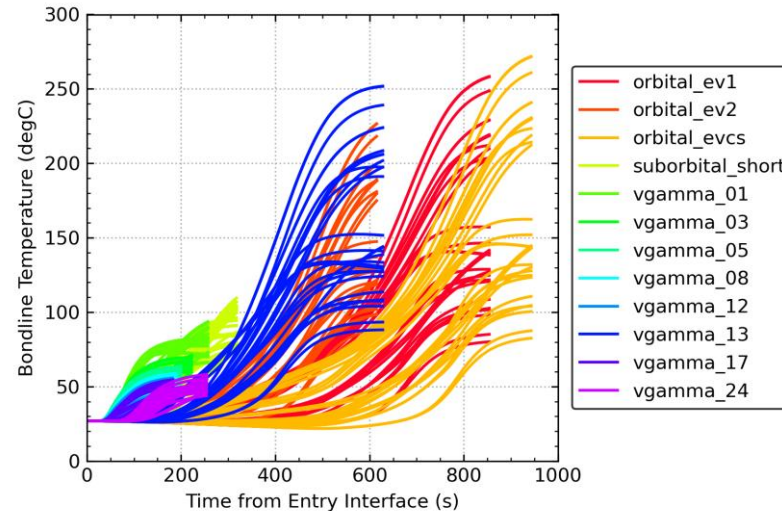
- Run FIAT for 30x different body points (8x different TPS stackups).
- Model incorporates pyrolysis and ablation.
- Predict the temperature at the TPS backface (aka the Bondline).
- Use standard suite of TPS modeling assumptions.

FIAT Assumptions

- 1D heat transfer.
- 240 K ambient re-radiation temp.
- Adiabatic backface.
- 300 K initial TPS temp (conservative).
- No ablation when $T_{\text{wall}} < 500$ K.
- Blowing parameter $\lambda=0.5$ when laminar, $\lambda=0.3$ when turbulent.



Sample TPS Stackup with Material Response Modeling Assumptions



Preliminary Bondline Temperatures ($\alpha = 0^\circ$)

TFAWS 2025 – August 4-7, 2025



Material Response Modeling



Send CBAERO heating to the material response solver FIAT [8].

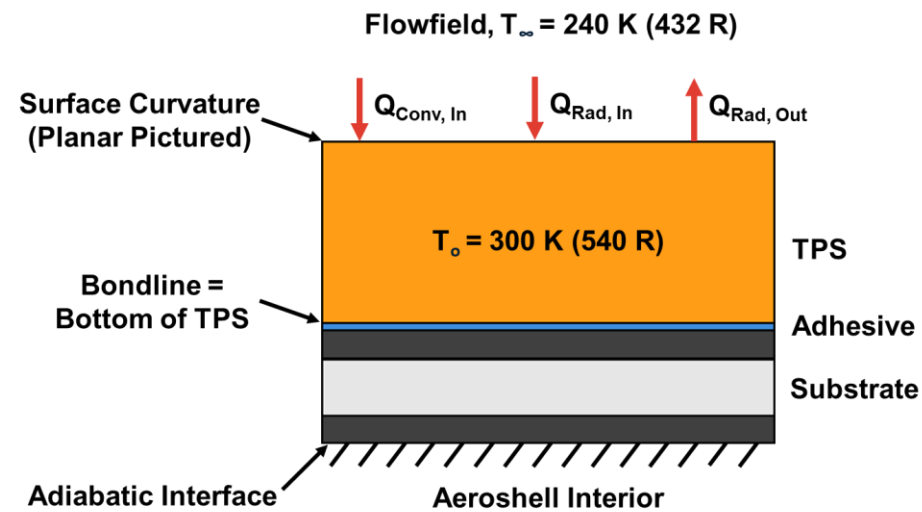
- Run FIAT for 30x different body points (8x different TPS stackups).
- Model incorporates pyrolysis and ablation.
- Predict the temperature at the TPS backface (aka the Bondline).
- Use standard suite of TPS modeling assumptions

Analysis is most sensitive to the starting TPS temperature.

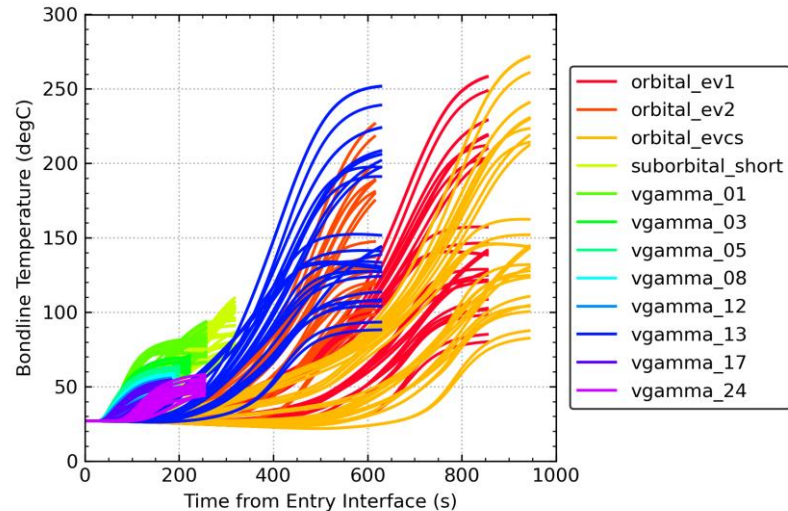
- Use a conservative value of 300 K; To be finalized.

FIAT Assumptions

- 1D heat transfer.
- 240 K ambient re-radiation temp.
- Adiabatic backface.
- 300 K initial TPS temp (conservative).
- No ablation when $T_{Wall} < 500$ K.
- Blowing parameter $\lambda=0.5$ when laminar, $\lambda=0.3$ when turbulent.

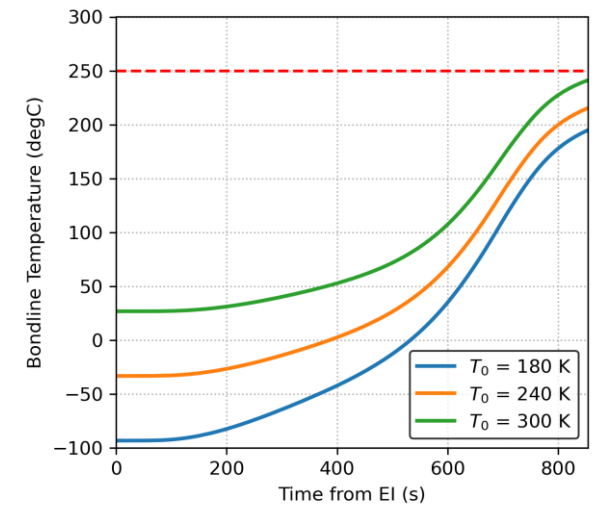


Sample TPS Stackup with Material Response Modeling Assumptions



Preliminary Bondline Temperatures ($\alpha = 0^\circ$)

TFAWS 2025 – August 4-7, 2025



Impact of Initial TPS Temperature on Bondline Temperature (Stag, $\alpha = 0^\circ$)



Summary & Next Steps



Dragonfly mission aerothermal team has developed an accidental Earth re-entry database.

- **Large CFD database of 84x cases covering the full range of angles of attack.**
- **Constructed with flight-heritage entry modeling tools (CBAERO, DPLR, FIAT).**
- **Radiation prediction coverage enabled by emerging tool NERO.**
- **More sophisticated than previous attempts to evaluate past assumptions.**

Preliminary results indicate minor bondline temperature exceedance for LEO-decay scenarios.

- **Currently verifying cases and determining impact of angle of attack oscillations.**

Next Steps:

- **Evaluate efficacy of past methods in accounting for Angle of Attack variation.**
- **Use the database to evaluate tumbling cases (EGA case may tumble).**
- **Develop a data-fusion methodology for real-time Radioisotope Contingency Planning.**



References



- [1] Shockley, S. (2023). *Literature Review: Safety Review Process for Space Nuclear System Launches*. Nuclear Regulatory Commission Research Information Letter 2023-06.
- [2] McQuaide, M., et al. (2023). *Dragonfly Phase B Mission Design*. AAS/AIAA Astrodynamics Specialist Conference, 13-17 August, Big Sky, MT.
- [3] Kinney, D. (2007). *Aerothermal Anchoring of CBAERO Using High Fidelity CFD*. AIAA Aerospace Sciences Meeting and Exhibit, 8-11 January, Reno, Nevada.
- [4] Mansour, N. N., et al. (2010). *Mars Science Laboratory Aeroshell CFD Analysis and Bondline Temperature Accidental Earth Reentry Study Final Report*. UNPUBLISHED: Internal Report.
- [5] Wright, M., et al. (1998). *Data-Parallel Line Relaxation Method for the Navier-Stokes Equations*. AIAA Journal, Vol. 36, No. 9, September.
- [6] Hollis, B. (2012). *Blunt-Body Entry Vehicle Aerothermodynamics: Transition and Turbulent Heating*. Journal of Spacecraft and Rockets, Vol. 49, No 3, May-June.
- [7] Sahai, A. and Johnston, C. (2023). *On Computationally Efficient Radiative Transfer Calculations for Three-dimensional Entry Problems*. AIAA Scitech Forum, 23-27 January, National Harbor, MD.
- [8] Chen, Y. K., and Milos, F. S. (1999). *Ablation and Thermal Response Program for Spacecraft Heatshield Analysis*. Journal of Spacecraft and Rockets, Vol. 36, No. 3, May-June.



QUESTIONS?



BACKUP

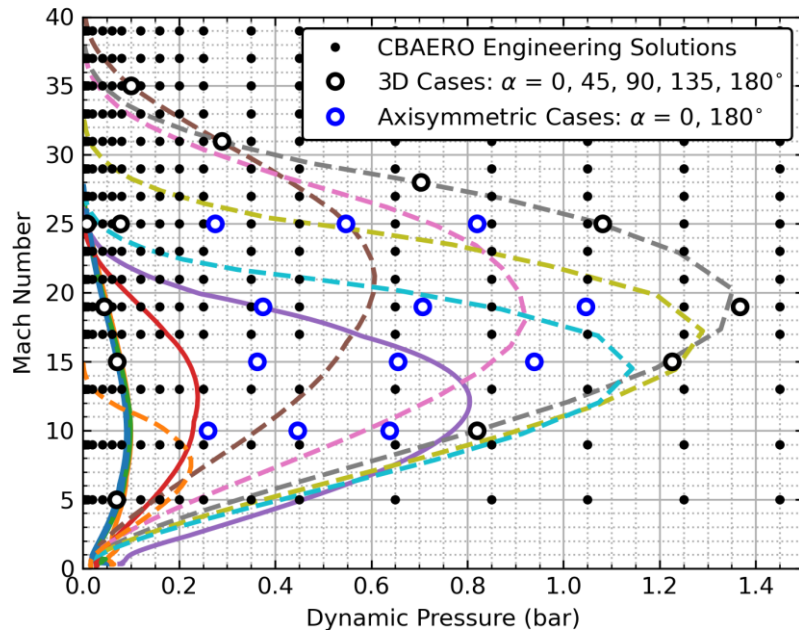


Aerothermal Database - CBAERO

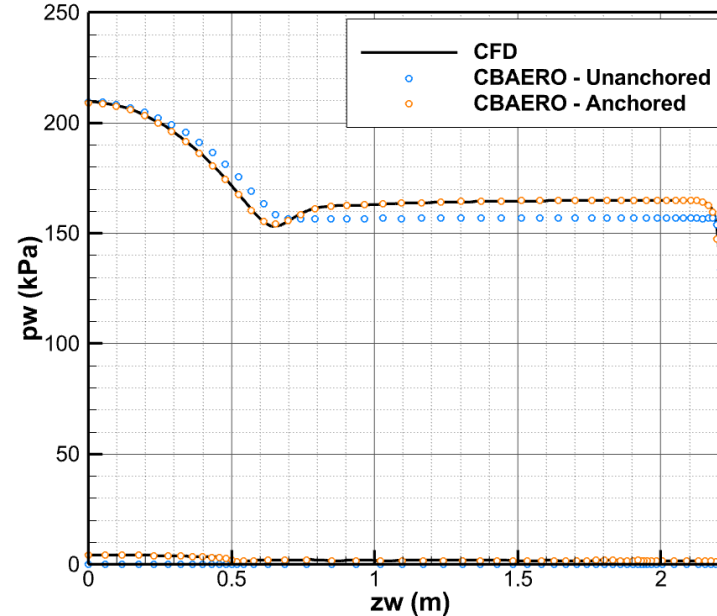


CBAERO is a common engineering tool for aerothermal design.

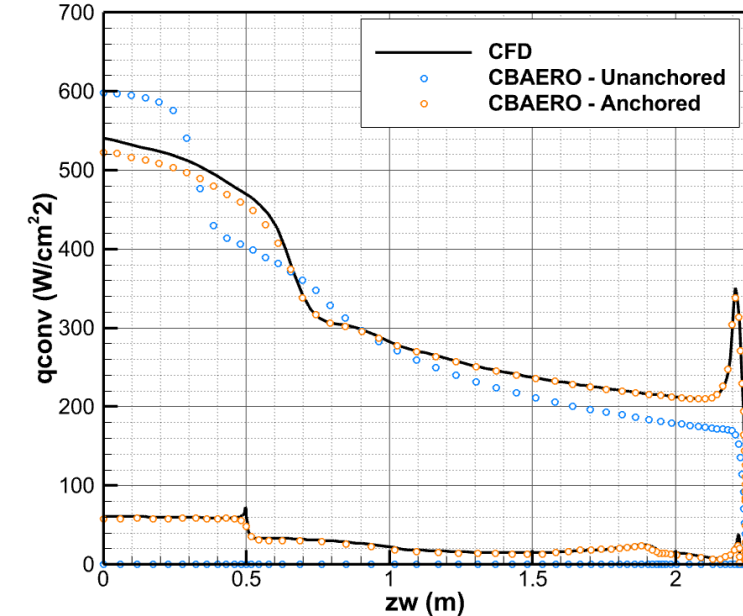
- Linearly interpolates within engineering solutions (cheap to produce).
- Corrects engineering solutions with high-fidelity CFD.
- Used by previous launch failure analyses (e.g., MSL [4]).



Trajectories in CBAERO Interpolation Space w/ High-Fidelity CFD



CBAERO Solutions With and Without Anchoring to CFD
($U_\infty = 7995 \text{ m/s}$, $\rho_\infty = 3.384 \times 10^{-3} \text{ kg/m}^3$)





Database CFD Conditions



Table of Database CFD Conditions (Ordered by U_∞)

Case ID	Altitude (km)	Mach	Dynamic Pressure (bars)	Total Angles of Attack (deg)	Velocity (m/s)	Density (kg/m ³)	Temperature (K)
3.1	64.54	35	1.004e-01	0, 45, 90, 135, 180	10745	1.740e-04	234.56
3.2	55.44	31	2.889e-01	0, 45, 90, 135, 180	10003	5.774e-04	259.19
3.3	47.06	28	7.034e-01	0, 45, 90, 135, 180	9167	1.674e-03	266.71
5.1	46.80	25	5.463e-01	0,180	8181	1.632e-03	266.49
4.1	52.25	25	2.747e-01	0,180	8177	8.219e-04	266.20
6.1	43.68	25	8.196e-01	0,180	8089	2.506e-03	260.52
2.1	41.50	25	1.081e+00	0, 45, 90, 135, 180	7995	3.384e-03	254.48
0.1	60.23	25	7.799e-02	0, 45, 90, 135, 180	7173	3.032e-04	204.86
1.1	76.82	25	7.799e-03	0, 45, 90, 135, 180	7173	3.032e-05	204.86
4.2	45.09	19	3.745e-01	0,180	6192	1.954e-03	264.28
5.2	40.30	19	7.063e-01	0,180	6037	3.877e-03	251.19
6.2	37.87	19	1.047e+00	0,180	5955	5.904e-03	244.44
1.2	61.79	19	4.370e-02	0, 45, 90, 135, 180	5926	2.489e-04	242.10
2.2	35.82	19	1.367e+00	0, 45, 90, 135, 180	5889	7.882e-03	238.88
1.3	54.97	15	7.084e-02	0, 45, 90, 135, 180	4856	6.009e-04	260.79
4.3	42.14	15	3.626e-01	0,180	4813	3.130e-03	256.27
5.3	37.84	15	6.550e-01	0,180	4700	5.930e-03	244.36
6.3	34.84	15	9.384e-01	0,180	4621	8.788e-03	236.18
2.3	33.28	15	1.226e+00	0, 45, 90, 135, 180	4591	1.163e-02	233.08
4.4	38.60	10	2.599e-01	0,180	3147	5.248e-03	246.48
5.4	34.51	10	4.468e-01	0,180	3077	9.441e-03	235.53
6.4	32.35	10	6.375e-01	0,180	3048	1.372e-02	231.22
2.4	30.44	10	8.203e-01	0, 45, 90, 135, 180	3023	1.795e-02	227.39
1.4	37.87	5	6.978e-02	0, 45, 90, 135, 180	1567	5.684e-03	244.45

Rad Cases
Bolded



CBAERO Grid

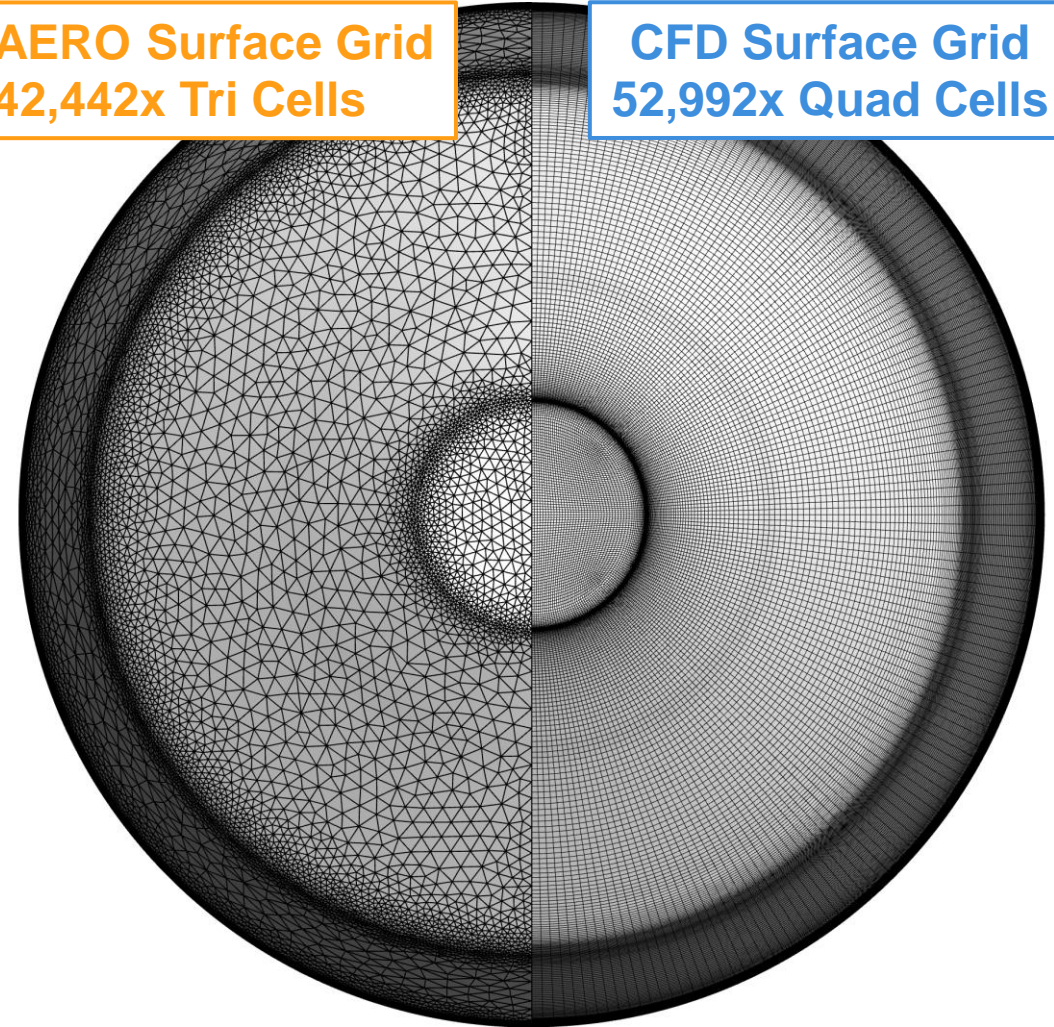
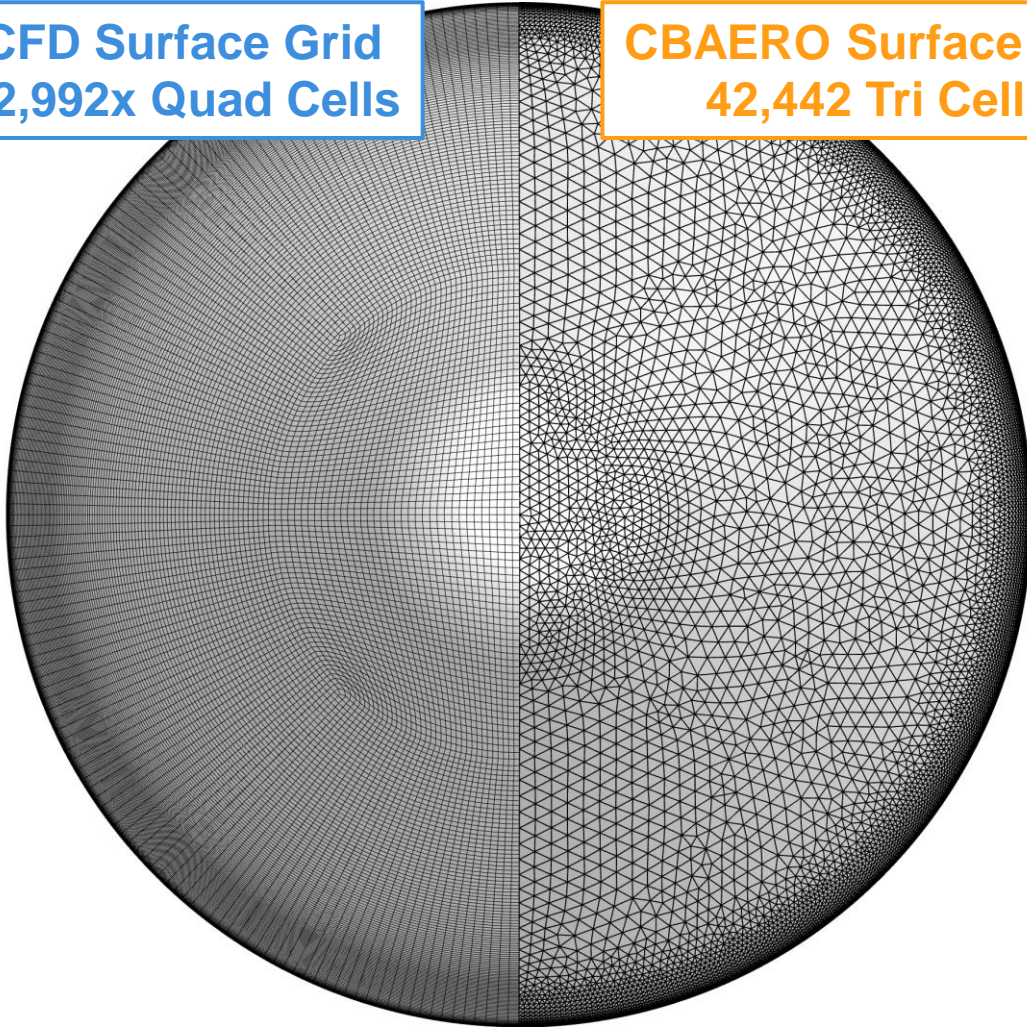


CFD Surface Grid
52,992x Quad Cells

CBAERO Surface Grid
42,442 Tri Cells

CBAERO Surface Grid
42,442x Tri Cells

CFD Surface Grid
52,992x Quad Cells





Radiative Heating – Code Validation

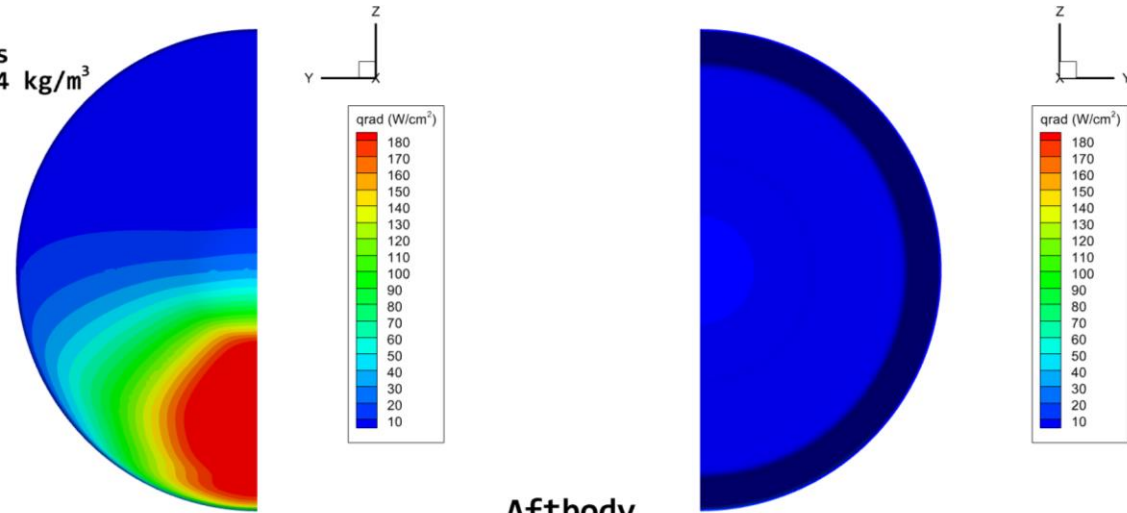


Validated NERO results with NEQAIR across freestream conditions and angles of attack.

- NERO underpredicts NEQAIR at large Qrad.
- Agreement is best for large Qrad.

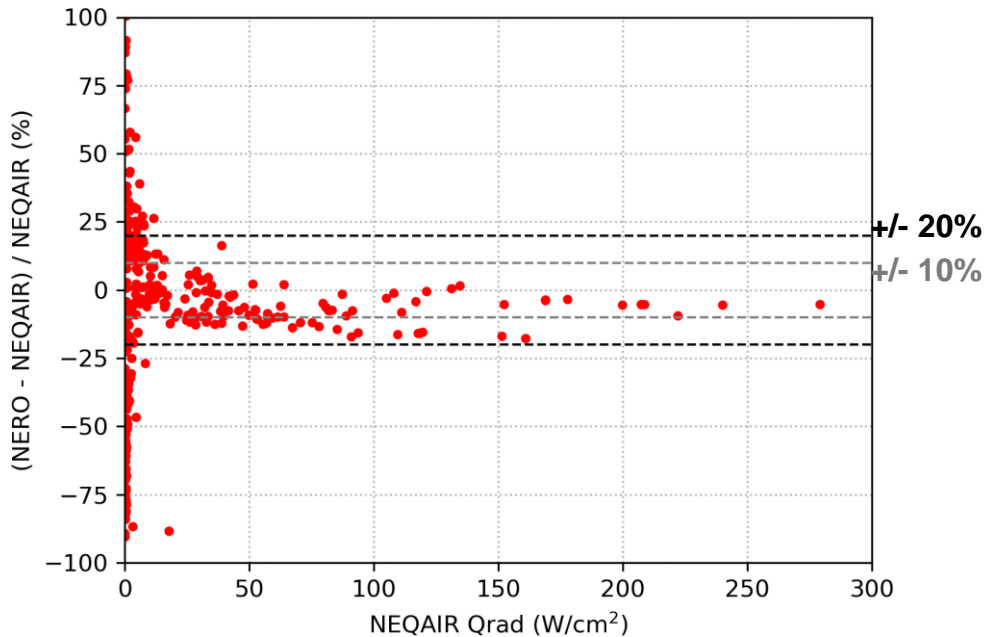
NERO is within 20% of NEQAIR for areas of relevant Qrad – Sufficient for database.

Case 3.1:
 $U = 10745 \text{ m/s}$
 $\rho = 1.740\text{e-}04 \text{ kg/m}^3$
 $\alpha = 45^\circ$



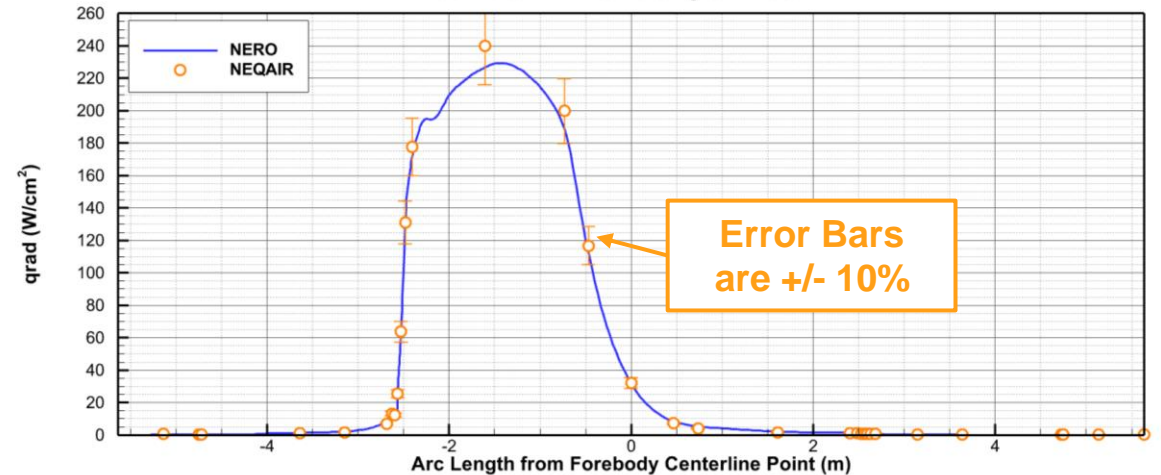
Forebody

Aftbody



Sample NERO and CFD Forebody Heating Contours

Centerline Comparison



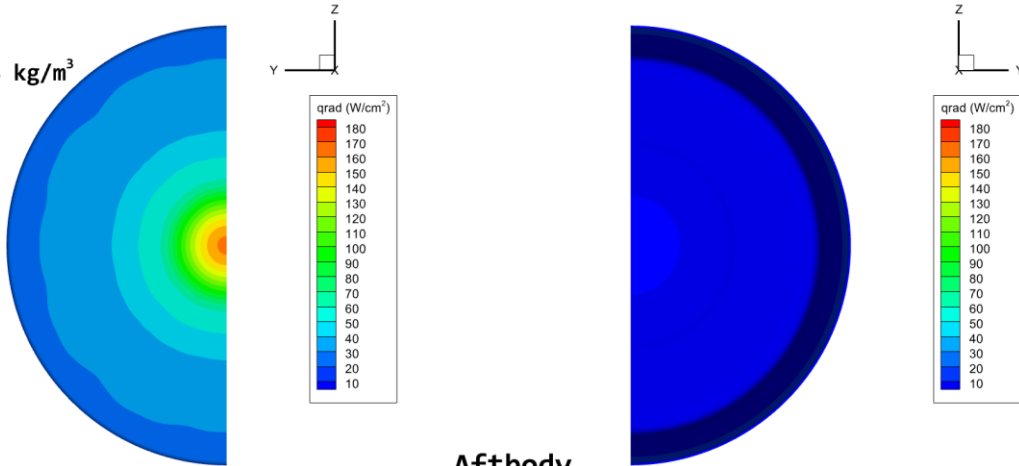
NERO & NEQAIR Hemisphere Comparison



Radiative Heating Validation – Case 3.1



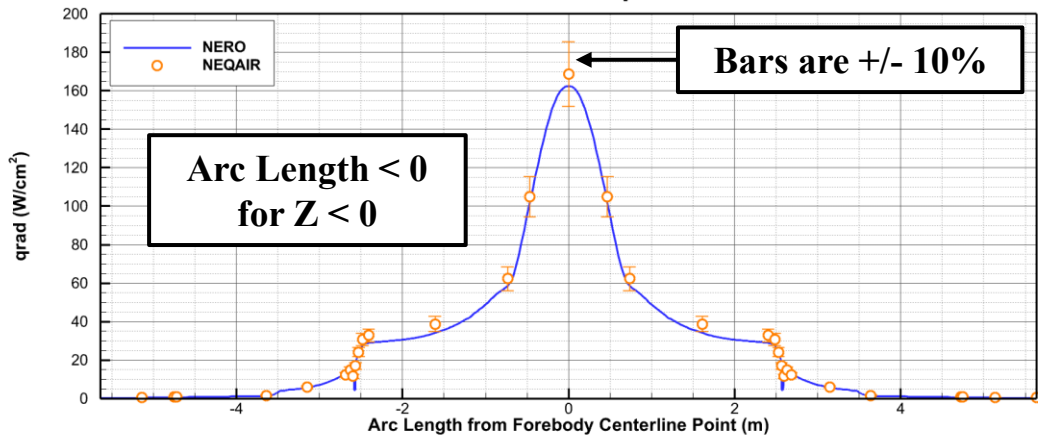
Case 3.1:
 $U = 10745 \text{ m/s}$
 $\rho = 1.740\text{e-}04 \text{ kg/m}^3$
 $\alpha = 0^\circ$



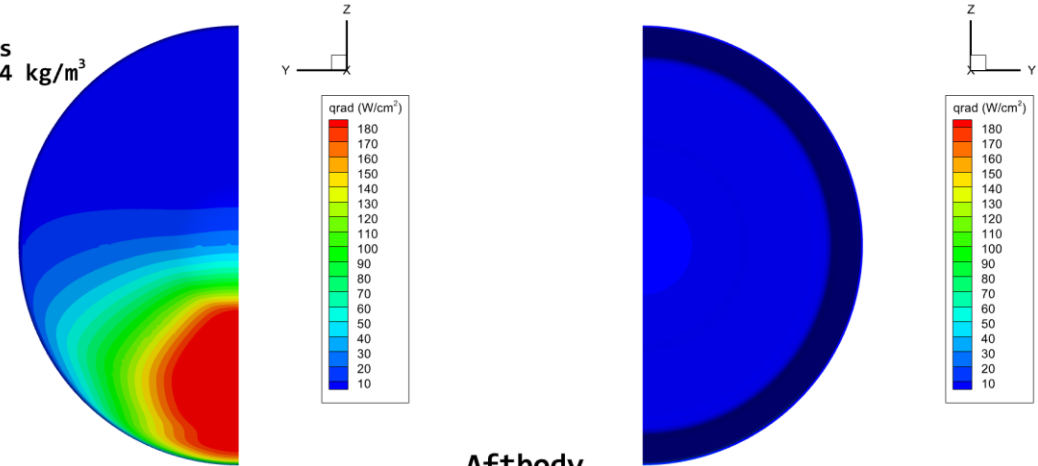
Forebody

Aftbody

Centerline Comparison



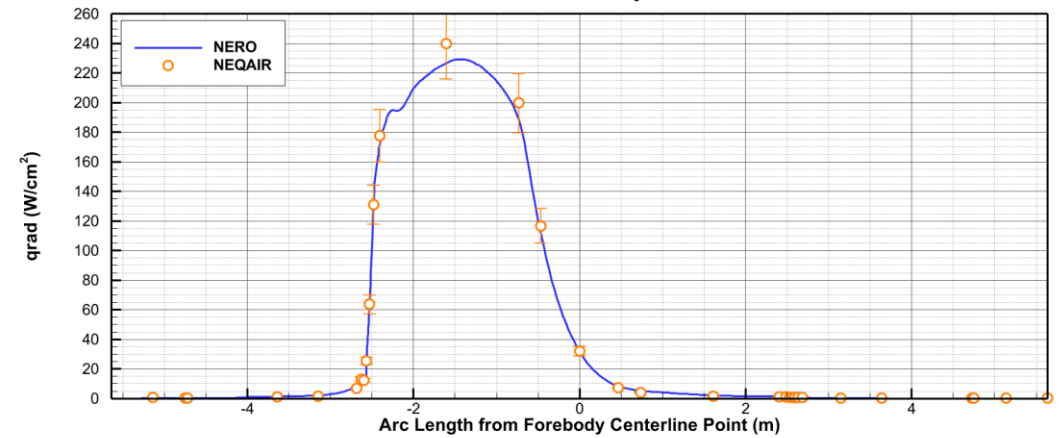
Case 3.1:
 $U = 10745 \text{ m/s}$
 $\rho = 1.740\text{e-}04 \text{ kg/m}^3$
 $\alpha = 45^\circ$



Forebody

Aftbody

Centerline Comparison

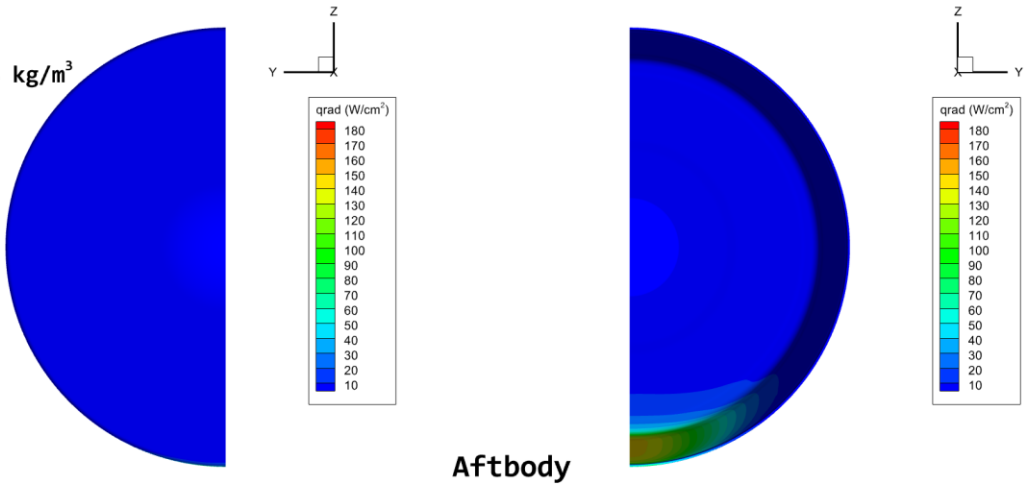




Radiative Heating Validation – Case 3.1



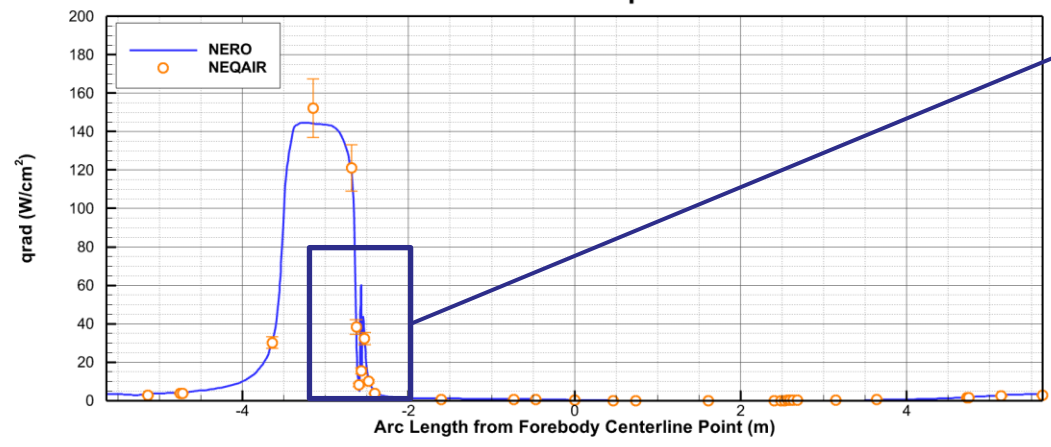
Case 3.1:
 $U = 10745 \text{ m/s}$
 $\rho = 1.740\text{e-}04 \text{ kg/m}^3$
 $\alpha = 90^\circ$



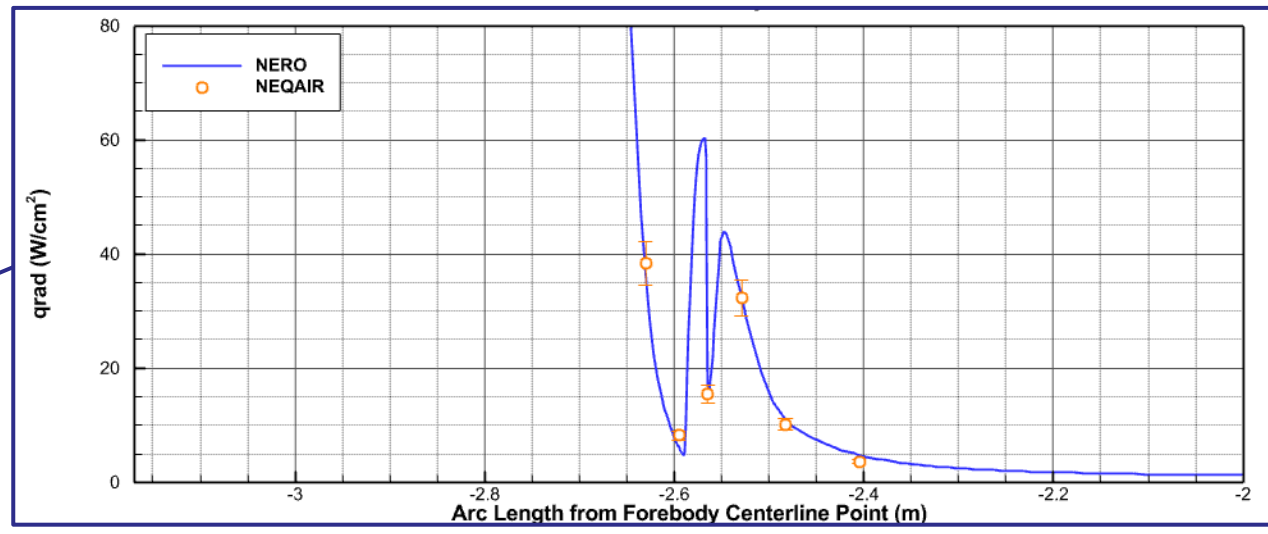
Forebody

Aftbody

Centerline Comparison



Zoom-In on Windside Aftbody Shoulder

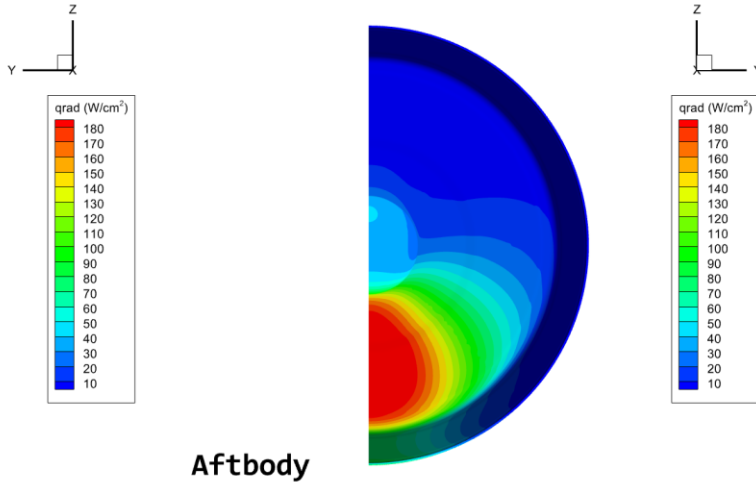




Radiative Heating Validation – Case 3.1



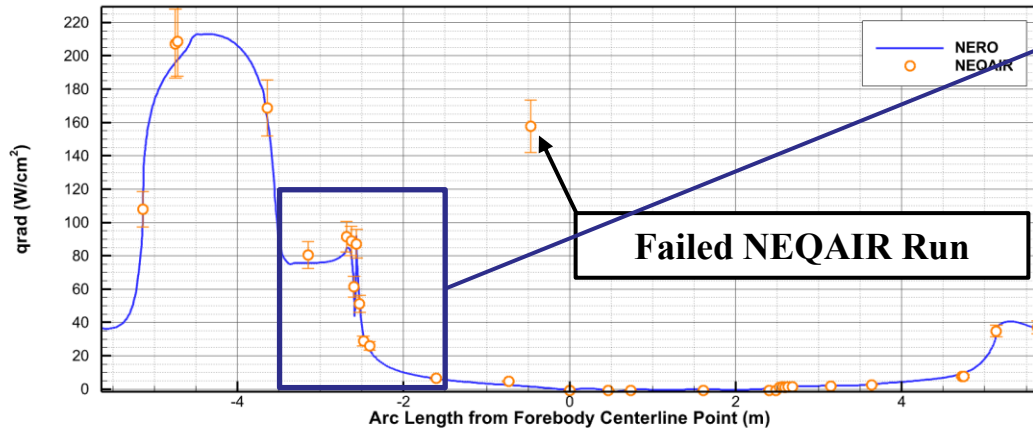
Case 3.1:
 $U = 10745 \text{ m/s}$
 $\rho = 1.740\text{e-}04 \text{ kg/m}^3$
 $\alpha = 135^\circ$



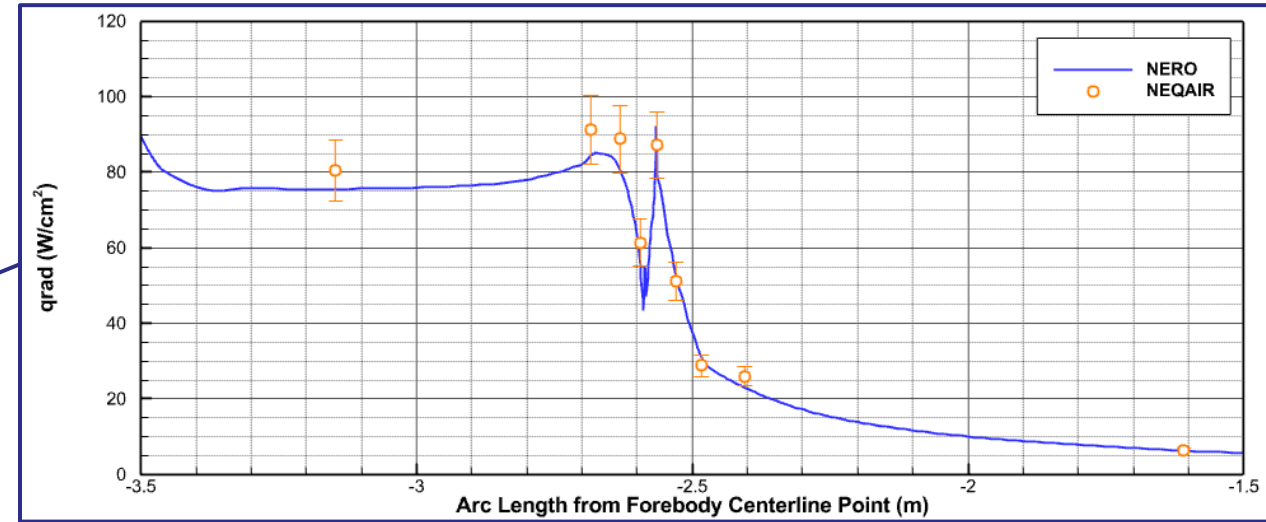
Forebody

Aftbody

Centerline Comparison

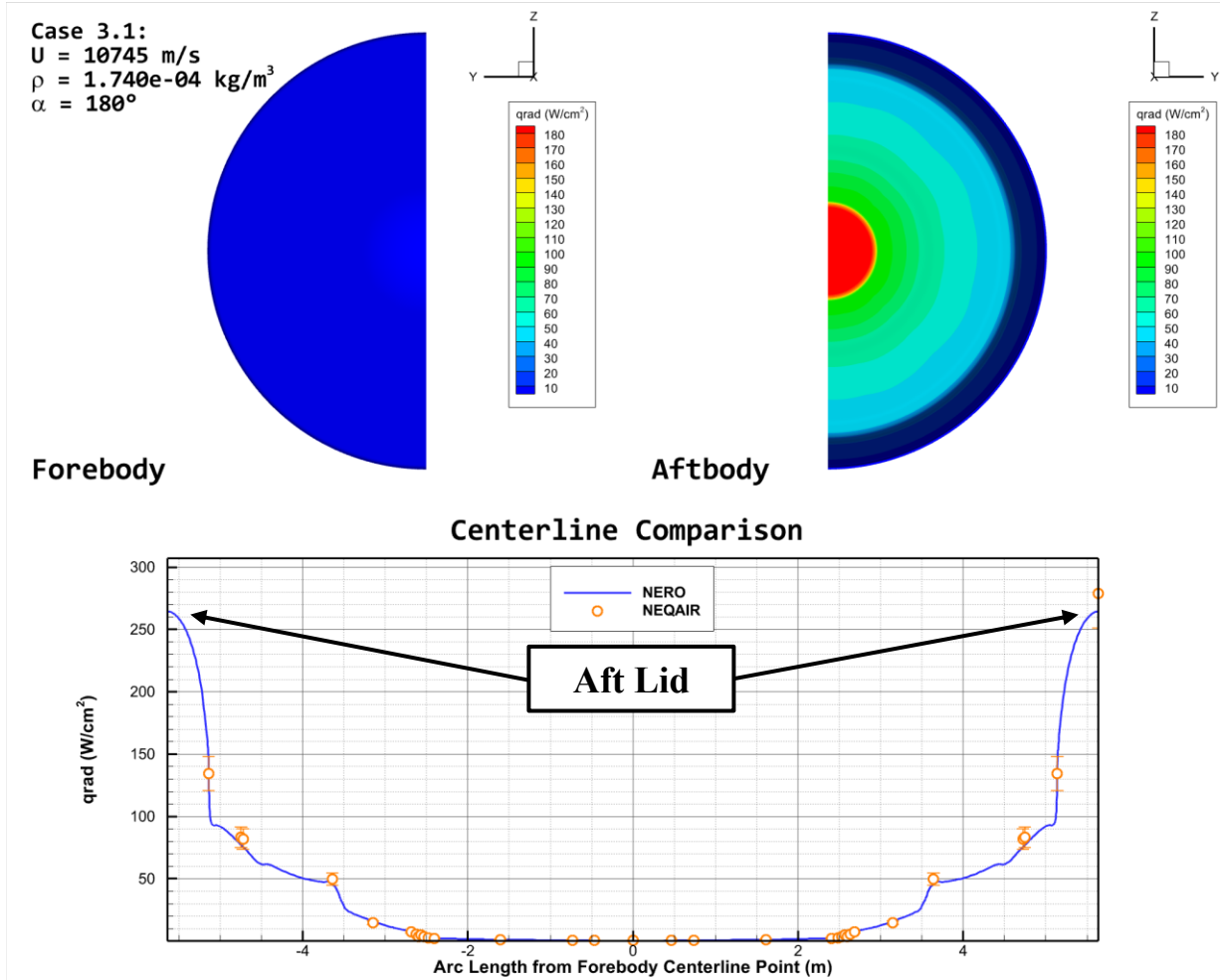


Zoom-In on Windside Aftbody Shoulder





Radiative Heating Validation – Case 3.1

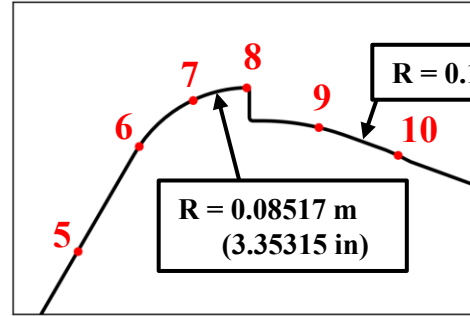




Selected Body Points

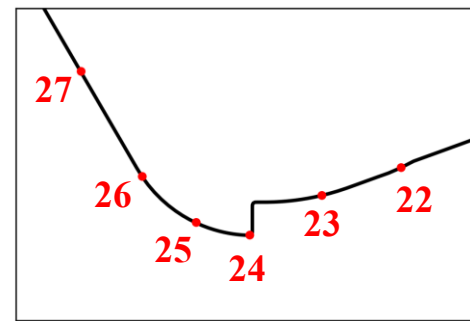


BP ID	xw (m)	yw (m)	zw (m)	Description	TPS Zone
1	0.00000	0.00000	0.00000	Stag point	1.2
2	0.08309	0.00000	0.45731	Windward stag at alpha=20deg	1.2
3	0.20113	0.00000	0.69639	Windward nose-flank tangency	1.0
4	0.64081	0.00000	1.45183	Windward mid-flank	1.0
5	1.04150	0.00000	2.14030	Windward zone 1 end	1.0
6	1.08082	0.00000	2.20750	Windward flank-sh tangency	2.0
7	1.11542	0.00000	2.23714	Windward mid shoulder	2.1
8	1.14983	0.00000	2.24512	Windward max diameter	2.1
9	1.19585	0.00000	2.21963	Windward aft shoulder	3.1
10	1.24665	0.00000	2.20187	Windward zone 4 start	4.0
11	1.68103	0.00000	2.04259	Windward zone 5 start	5.0
12	2.10086	0.00000	1.81547	Windward conic interface end	5.0
13	2.61745	0.00000	0.86410	Windward zone 5 end	5.0
14	2.62800	0.00000	0.84459	Windward zone 6 start	6.0
15	2.81385	0.00000	0.49838	Windward lid edge	7.0
16	2.81385	0.00000	0.00000	Lid center	8.0
17	2.81385	0.00000	-0.49838	Leeward lid edge	7.0
18	2.62800	0.00000	-0.84459	Leeward zone 6 start	6.0
19	2.61745	0.00000	-0.86410	Leeward zone 5 end	5.0
20	2.10086	0.00000	-1.81547	Leeward conic interface end	5.0
21	1.68103	0.00000	-2.04259	Leeward zone 5 start	5.0
22	1.24665	0.00000	-2.20187	Leeward zone 4 start	4.0
23	1.19585	0.00000	-2.21963	Leeward aft shoulder	3.1
24	1.14983	0.00000	-2.24512	Leeward max diameter	2.1
25	1.11542	0.00000	-2.23714	Leeward mid shoulder	2.1
26	1.08082	0.00000	-2.20750	Leeward flank-sh tangency	2.0
27	1.04150	0.00000	-2.14030	Leeward zone 1 end	1.0
28	0.64081	0.00000	-1.45183	Leeward mid-flank	1.0
29	0.20113	0.00000	-0.69639	Leeward nose-flank tangency	1.0
30	0.08309	0.00000	-0.45731	Leeward stag at alpha=20deg	1.2

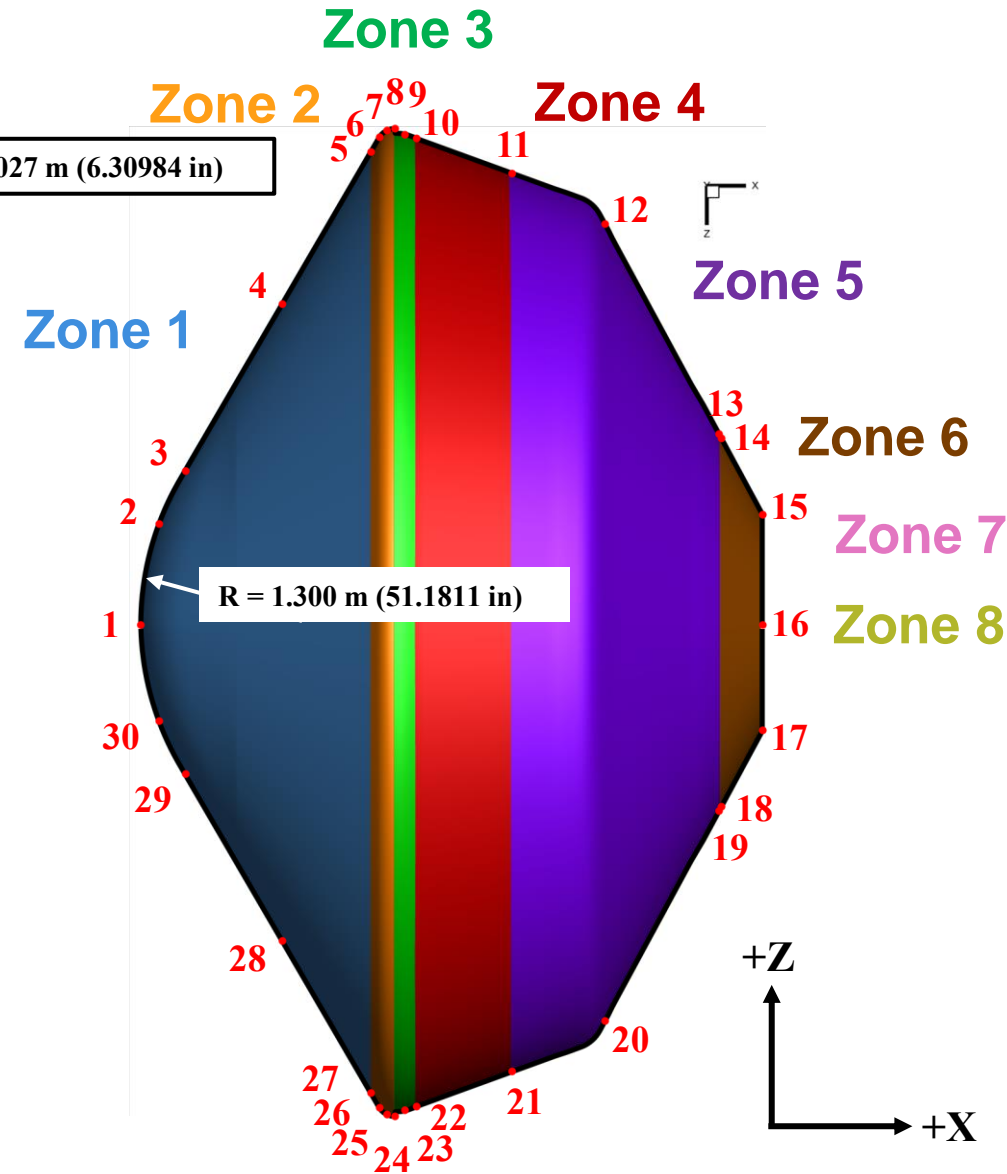


Windside Shoulder

NOTE: "TPS Zone" consists of two digits. The first digit defines the TPS stackup zone and the second digit describes the surface curvature (0 = Planar, 1=Cylindrical, 2=Spherical).



Leaside Shoulder





Radiative Heating – Flight Space

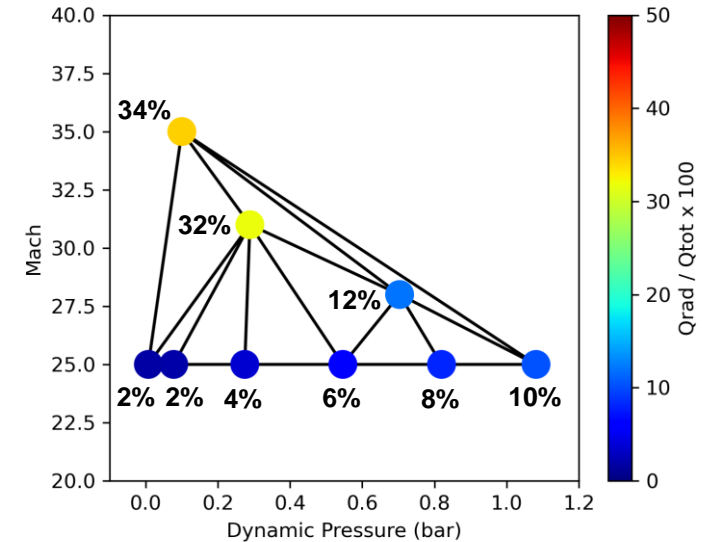
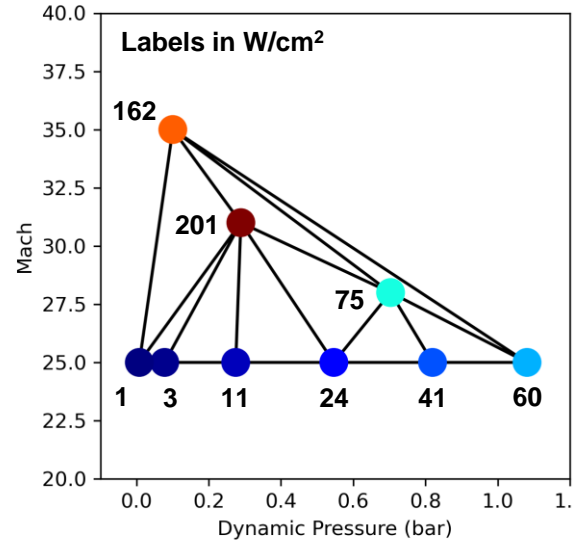


Radiative heat flux is a significant portion of the heat pulse for EGA entries.

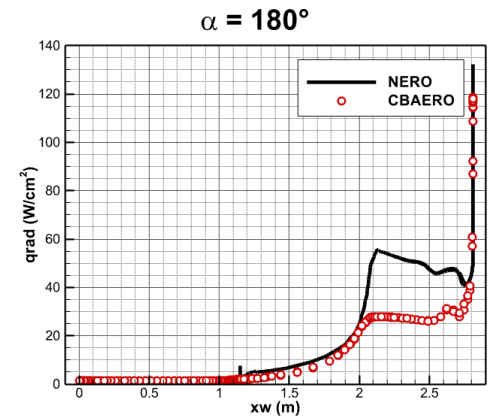
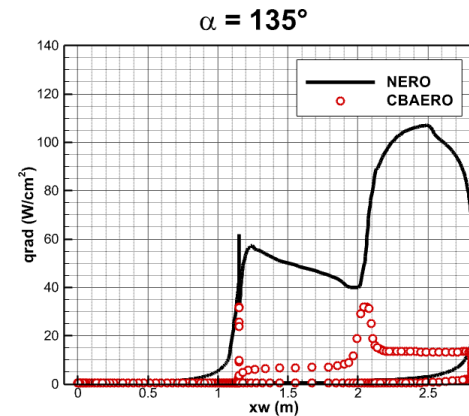
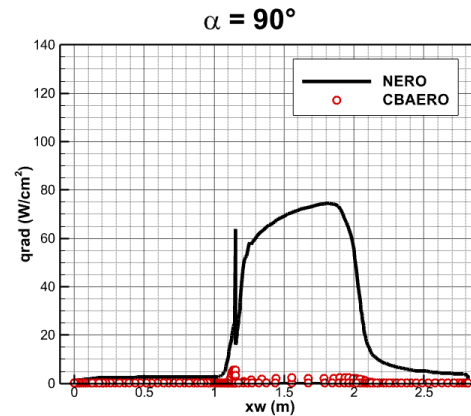
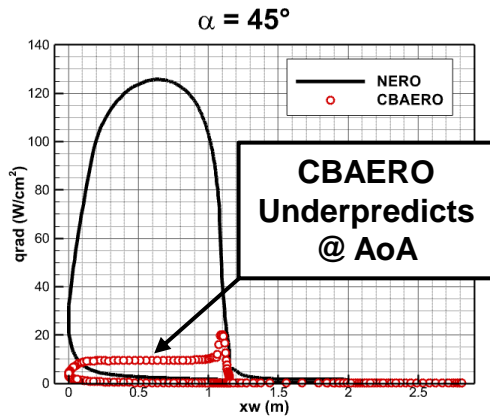
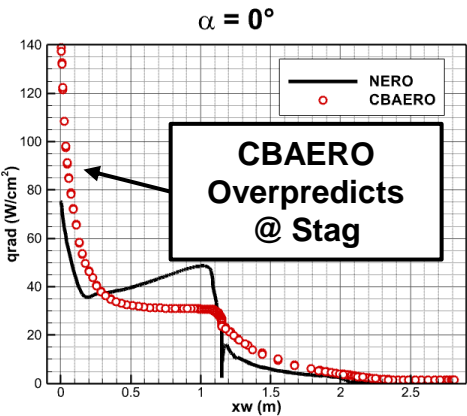
- Makes up ~30% of early total heating.
- Becomes insignificant by $U_\infty \approx 7$ km/s; Database has sufficient coverage.

CBAERO predictions are decent at $\alpha = [0^\circ, 180^\circ]$ and poor at $\alpha = [45^\circ, 90^\circ, 135^\circ]$.

Qrad anchoring likely unnecessary for $\alpha = [0^\circ, 180^\circ]$ but important for other α 's.



Stag-Point Radiative Heating and % of Total Heat Flux ($\alpha = 0^\circ$)

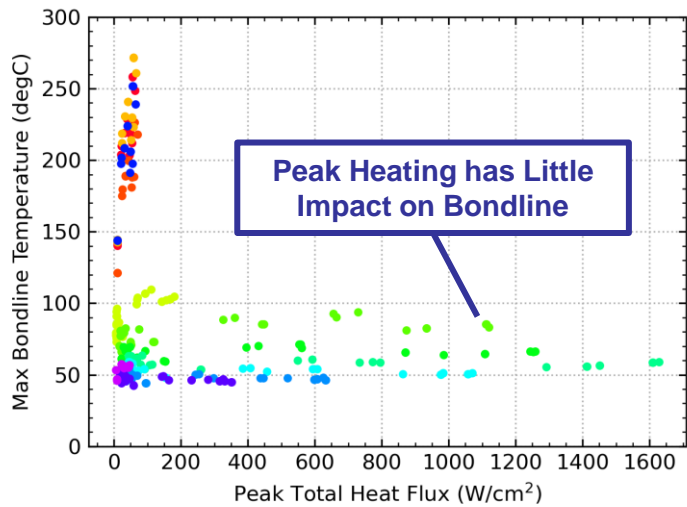
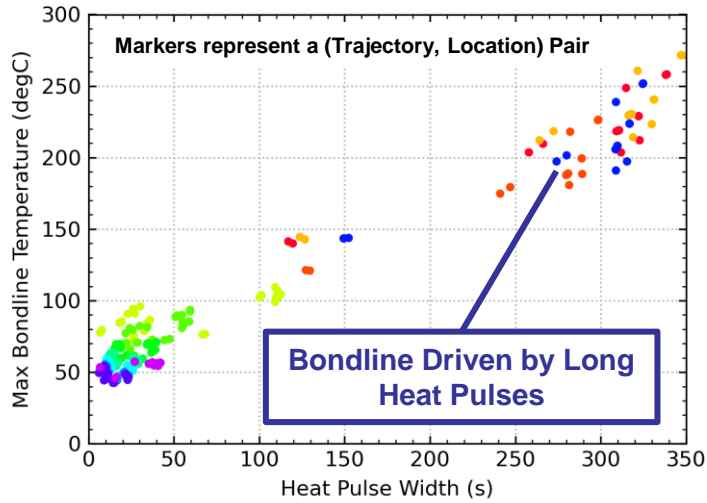


Wall Heat Flux Contours at Database Angles of Attack ($U_\infty = 9167$ m/s, $\rho_\infty = 1.674 \times 10^{-3}$ kg/m³)

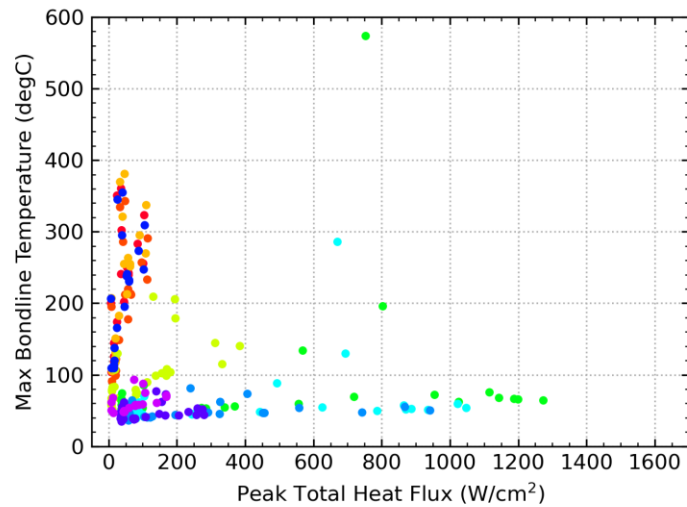
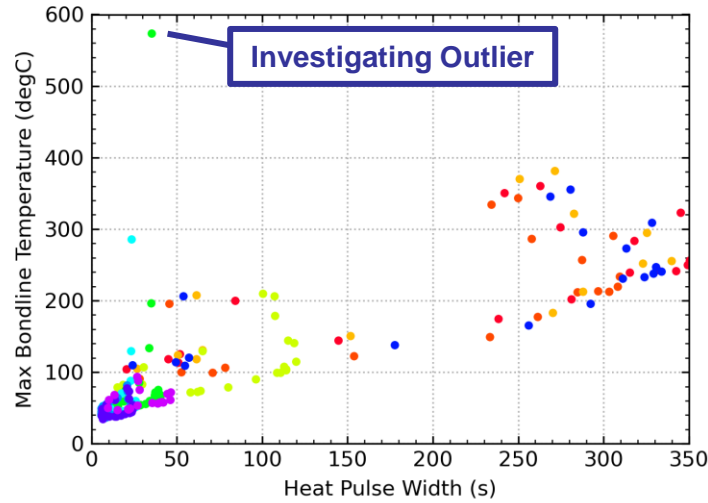


Preliminary Results

$\alpha = 0^\circ$

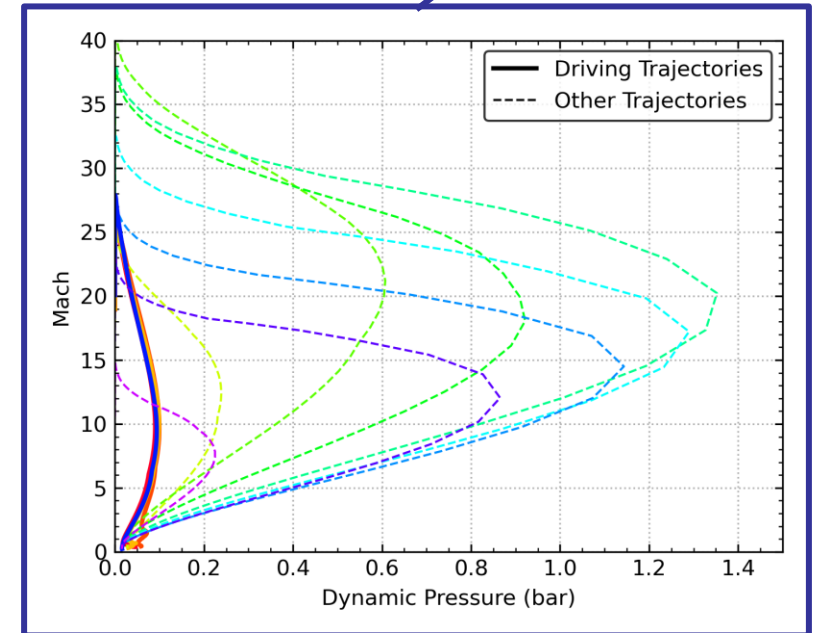


$\alpha = 45^\circ$



- orbital_ev1
- orbital_ev2
- orbital_evcs
- suborbital_short
- vgamma_01
- vgamma_03
- vgamma_05
- vgamma_08
- vgamma_12
- vgamma_13
- vgamma_17
- vgamma_24

Driving Trajectories all look like Orbital decay.



Heat Pulse Characteristics for Preliminary Trajectories